Published in final edited form as:

Cell Death Differ. 2010 December ; 17(12): 1867–1881. doi:10.1038/cdd.2010.53.

ARSENIC TRIOXIDE INDUCES A BECLIN-1 INDEPENDENT AUTOPHAGIC PATHWAY VIA MODULATION OF SNON/SKIL EXPRESSION IN OVARIAN CARCINOMA CELLS

Dawn Smith[1], **Shetal Patel**[1], **Fadi Raffoul**[1], **Edward Haller**[2], **Gordon B. Mills**[3], and **Meera Nanjundan**[1,*]

[1]University of South Florida, Department of Cell Biology, Microbiology, and Molecular Biology, 4202 East Fowler Avenue, BSF218, Tampa, Florida

[2]University of South Florida, Department of Integrative Biology, 4202 East Fowler Avenue, Tampa, Florida

[3]University of Texas, MD Anderson Cancer Center, Department of Systems Biology, 1515 Holcombe Boulevard, Box 950, Houston, Texas

Abstract

Arsenic trioxide (As_2O_3), used to treat promyelocytic leukemia, triggers cell death via unknown mechanisms. To further our understanding of As_2O_3-induced death, we investigated its effects on transforming growth factor-β (TGFβ) signaling mediators in ovarian cells. Dysregulated TGFβ signaling is a characteristic of ovarian cancers. As_2O_3 reduced the protein expression of EVI1, TAK1, SMAD2/3, and TGFβRII while increasing SnoN/SkiL. EVI1 protein was modulated by treatment with the proteosome inhibitors, MG132 and PS-341/Velcade, suggesting that degradation occurs via the ubiquitin-proteosome pathway. The sensitivity of ovarian cells to As_2O_3–induced apoptosis correlated with expression of multidrug resistance protein 1. Interestingly, expression of SnoN was similar to LC3-II (autophagy marker) which increased with induction of cytoplasmic vacuolation preceding apoptosis. These vesicles were identified as autophagosomes based on transmission electron microscopy and immunofluorescence staining with EGFP-LC3. The addition of N-acetyl-L-cysteine (ROS scavenger) to As_2O_3-treated cells reversed changes in SnoN protein and the autophagic/apoptotic response. In contrast to Beclin-1 knockdown, siRNA targeting ATG5, ATG7, and hVps34 markedly reduced autophagy in As_2O_3-treated ovarian carcinoma cells. Further, treatment with SnoN siRNA markedly decreased LC3-II levels and increased PARP degradation (an apoptosis marker). Collectively, these findings suggest that As_2O_3 induces a Beclin-1 independent autophagic pathway in ovarian carcinoma cells and implicates SnoN in promoting As_2O_3-mediated autophagic cell survival.

[*]**Corresponding Author:** Meera Nanjundan, 4202 East Fowler Avenue, BSF218, Department of Cell Biology, Microbiology, and Molecular Biology, University of South Florida, Tampa, Florida, 33620, Phone: 813-974-8133; Fax: 813-974-1614, mnanjund@usf.edu.

Conflict of Interest. The authors declare no conflict of interest.

Keywords

ovarian cancer; ecotropic viral integration site-1 (EVI1); SnoN/SkiL; transforming growth factor-β (TGFβ); arsenic trioxide (As_2O_3); apoptosis; autophagy; reactive oxygen species (ROS); multidrug resistance protein (MRP1)

Introduction

Ovarian cancer is the 5th most common cancer in women with approximately 22,000 new cases and 15,000 deaths each year in the United States based on National Cancer Institute statistics. Although advances in surgery and chemotherapy have improved the survival rate, the development of resistance to chemotherapy continues to be a challenging clinical problem in the treatment of advanced stage ovarian carcinoma. Thus, greater effort is needed to identify novel therapeutic targets and treatment strategies. Targeting signaling pathways that are dysregulated in cancer, such as those mediated by transforming growth factor-beta (TGFβ), is one approach to improving patient survival. TGFβ mediates both tumor suppressing and tumor promoting activities by (1) repressing transformation in normal cells and (2) increasing aggressiveness of transformed cells through induction of epithelial-mesenchymal transition (EMT), which leads to increased invasion and metastases.1 TGFβ regulates target gene expression through SMAD-dependent and SMAD-independent pathways. Several TGFβ signaling mediators are altered during ovarian cancer development including ecotropic viral integration site-1 (EVI1),2, 3 SnoN/SkiL,4 and TGFβRII, and PI3K/AKT.1,3 In ovarian cancers, proposed mechanisms for resistance to TGFβ-mediated growth inhibition include decreased expression of TGFβ receptors, repression by oncoproteins (EVI1 and SnoN), dysregulation of RUNX1 activation, and activation of additional pathways such as PKC.1

Arsenic trioxide (As_2O_3), used in patients with acute promyelocytic leukemia (APL),5 is active *in vitro* in several solid tumor cell lines, including ovarian cancer cells.6–8 In human ovarian carcinoma cell lines, As_2O_3 is highly cytotoxic, inducing apoptosis, necrosis, autophagy, and inhibiting invasion.6, 8, 9 The mechanism of action of As_2O_3 is unclear. Interestingly, in primary murine leukemia cells, 2–10μM As_2O_3 is involved in proteosome degradation of EVI1, a well known TGFβ signaling repressor.10 To investigate the mechanism of drug-induced cell death, we examined the effects of As_2O_3 on TGFβ signaling mediators in ovarian cells. As_2O_3 markedly altered protein levels of EVI1, SnoN, TGFβRII, as well as other key TGFβ signaling mediators, including SMAD2/3 and AKT. EVI1 protein expression was restored by MG132/PS-341 treatment suggesting that As_2O_3 induced effects on EVI1 is regulated through the proteosome degradation pathway. As_2O_3 elicited a marked functional effect on cell growth and apoptosis in a number of ovarian cell lines which correlated with MRP1 protein expression. siRNA targeting ATG5, ATG7, and hVps34 markedly reduced autophagy in As_2O_3-treated ovarian carcinoma cells in contrast to Beclin-1 knockdown which had no effect implicating a Beclin-1 independent mechanism in As_2O_3–induced autophagy. Moreover, SnoN alters cellular sensitivity to apoptosis by modulating LC3-II levels. Our results implicate SnoN as a potential target for therapy since it promotes cell survival via modulation of autophagy and apoptosis.

Results

As_2O_3 alters expression of TGFβ signaling mediators in ovarian cancer cells

To determine the mechanism of action of As_2O_3 in ovarian cancer cell lines, we initially determined its effect on the expression of TGFβ signaling mediators including EVI1, which is amplified at 3q26.2 in ovarian cancers.2 We treated HEY and OVCA429 cells (high EVI1 expressing cell lines) for 18 hours with increasing doses of As_2O_3 (Figure 1a and Supplementary Figure 1a). As_2O_3 markedly decreased protein levels of several EVI1 forms in both cell lines including MDS1/EVI1 (which consists of sequences derived from both EVI1 and the MDS1 gene, located telomeric to EVI1),11 full-length EVI1, and $EVI1^{Del190–515}$ (similar to the identified Δ324 isoform isolated from human endometrial carcinoma cells).12, 13 In contrast, As_2O_3 significantly increased SnoN/SkiL levels, also amplified at the 3q26.2 locus in ovarian cancers.4 Other TGFβ mediators markedly reduced by As_2O_3 treatment include (1) TGFβ activating kinase 1 (TAK1) which phosphorylates SnoN targeting it for degradation,14 (2) SMAD2/3, (3) TGFβRII which is down-regulated in advanced stage ovarian carcinomas relative to normal epithelium3 (western analysis shows multiple bands likely reflecting heterogeneity of the receptor), and (4) AKT, which can signal through the TGFβ pathway by binding to SMAD3.15 Thus, these data demonstrate that As_2O_3 markedly alters expression of key TGFβ signaling mediators in ovarian cancer cells.

As_2O_3 induces the degradation of TGFβ signaling mediators via proteosome-dependent and -independent pathways

To determine whether alterations in expression of TGFβ signaling mediators following treatment with As_2O_3 were due to proteosome-mediated degradation, we performed combinatorial studies with the proteosome inhibitor MG132. We used As_2O_3 at 5μM with 5μM MG132 which elicited minimal cellular toxicity compared to higher doses. The response of HEY and OVCA429 to these drug combinations were similar (Figure 1b and Supplementary Figure 1b). Both EVI1 and $EVI1^{Del190–515}$ protein expression were reduced with 5μM As_2O_3 while there was little effect on MDS1/EVI1 (Figure 1b).10 The reduction of EVI1 and $EVI1^{Del190–515}$ expression with As_2O_3 was recovered with the proteosome inhibitor MG132, suggesting that As_2O_3-induces the degradation of certain EVI1 forms through a proteosome-mediated pathway. In contrast, TGFβRII was not markedly recovered following 6 or 18 hour treatment with MG132, suggesting that As_2O_3-induced degradation of TGFβRII likely occurs via a proteosome-independent pathway. Strikingly, SnoN levels were further increased with MG132, suggesting that SnoN protein can be further stabilized via a proteosome-mediated pathway. Similar effects were observed with PS-341 (Bortezomid/Velcade), another proteosome inhibitor (Figure 1c).

SMURF2 (E3 ubiquitin ligase) is involved in geldanamycin-induced TGFβRII degradation. 16 However, treatment of OVCA429 and HEY ovarian cancer cells with SMURF2 siRNA (>90% reduction in SMURF2 protein) did not significantly alter EVI1, SnoN, or TGFβRII protein in the absence or presence of As_2O_3 (Supplementary Figure 1c) suggesting other E3 ubiquitin ligases are involved in As_2O_3-induced degradation of TGFβRII, SnoN, or EVI1.

We next assessed whether As_2O_3-induced alterations in AKT, SMAD2/3, and TGFβRII protein with MG132 were due to changes in (1) protein expression independent of the proteosome or (2) RNA levels. MG132 treatment at 18 hours not only significantly decreased their protein levels (Figure 1d and Supplementary Figure 1d), but markedly reduced EVI1 and TGFβRII RNA levels (Figure 1e and Supplementary Figure 1e). We also examined the effect of As_2O_3 on RNA levels (Figure 1e) since As_2O_3 can alter RNA expression such as survivin.17, 18 However, we observed <20% decrease in EVI1 and TGFβRII RNA levels with little effect on SnoN RNA. Collectively, these results suggest that As_2O_3-induced expression changes occurs mostly at the protein level.

Decreased sensitivity to As_2O_3–induced cell death in ovarian cells expressing high MRP1 protein

In order to examine the functional effects of As_2O_3 on both normal and ovarian cancer cells, we assessed its effects on cell growth in (1) T80, a large T antigen/hTERT immortalized normal ovarian surface epithelial cell line (low expressing EVI1 cell line), (2) HEY (moderate expressing EVI1 cell line), and (3) SKOV3, (high expressing EVI1 cell line).2 We previously reported the expression profile of EVI1 in these ovarian cells.2 High expressing EVI1 cells (HEY and SKOV3) were more resistant to effects of As_2O_3 compared to low EVI1 expressing cells (T80) based on cell viability assays (Figure 2a). Upon microscopic examination, we observed that these cells developed numerous cytoplasmic vacuoles and were apoptotic as evidenced by apoptotic morphology and substratum release (Figure 2b). Staining with annexin V-FITC and propidium iodide (PI) to quantify changes in apoptosis indicated that, following As_2O_3 treatment, normal ovarian cells (T80) had a markedly higher apoptotic percentage (>80%) compared to ovarian cancer cells (SKOV3 and HEY; <20%) (Figure 2c). These results indicate that normal ovarian cells (T80) are more sensitive to As_2O_3–induced apoptosis compared to cancer cells (HEY and SKOV3). In contrast, As_2O_3 reduced the migratory potential of both normal and cancer cell lines similarly by >50% (Supplementary Figure 2).

Since As_2O_3 has been reported to reduce intracellular glutathione (GSH) levels,19 we next assessed whether GSH levels in T80, HEY, and SKOV3 cells may be correlated with the sensitivity to As_2O_3. All cell lines had reduced GSH levels following As_2O_3 treatment with markedly reduced levels in normal immortalized ovarian T80 cells compared to HEY and SKOV3 (Figure 2d). Since GSH can bind to trivalent arsenic and is effluxed out of cells through the multidrug resistance protein 1 (MRP1),20 we thus investigated the level of MRP1 protein in these ovarian cell lines. Indeed, we found that MRP1 was highly expressed in SKOV3 and HEY cells (highly resistant to As_2O_3 mediated effects) and low in T80 cells (Figure 2e). Together, these results suggest that the decreased sensitivity to As_2O_3 in ovarian carcinoma cells may be due to increased efflux of GSH-As_2O_3 through MRP1.

As_2O_3 induces formation of autophagosomes

Since formation of cytoplasmic vacuoles with As_2O_3 treatment was suggestive of induction of autophagy (see Figure 2b), we first examined protein expression of microtubule-associated protein light chain 3 (LC3), a marker of autophagic vesicle formation. As_2O_3 increased levels of both the LC3-I (cytosolic form, 18kDa) and LC3-II (membrane-bound

form, 16kDa) which correlated with SnoN expression at 10–25μM in T80/HEY cells and >25μM in SKOV3 cells (Figure 3a). p62/SQSTM1, which recruits autophagic machinery to inclusion bodies as a protective response for clearing protein aggregates through the autophagic pathway,21 also increased in a dose-dependent manner. In addition, poly (ADP-ribose) polymerase (116kDa, PARP), which is proteolytically fragmented to 89 and 24kDa (early marker of apoptosis) by caspase-3 which precedes DNA fragmentation, dramatically increased at a dose of 25μM (T80) and 50μM (HEY and SKOV3) correlating with the apoptotic sensitivity determined by Annexin V staining (see Figure 2c).

Since the development of cytoplasmic vacuoles at 18 hours treatment preceded apoptosis as determined by light microscopy (Figure 3b), we performed a kinetic profile to follow these events in a time-dependent manner with respect to expression of TGFβ mediators (Figure 3c). We observed induction of SnoN at 9 hour As_2O_3 treatment which correlated with changes in LC3-II and p62. We observed dramatic decreases in EVI1, TAK1, SMAD2/3, TGFβRII expression levels at 18 hours treatment which correlated with marked increases in the LC3-I/II ratio as well as reduction in procaspase-3 and increased cleaved PARP. Induction of another potential splice variant of EVI1 (~60kDa, detected using an antibody which detects multiple splice forms of EVI1) followed levels of cleaved PARP. These results provide evidence for the correlation of the induction of expression of SnoN with the autophagic marker, LC3-II, which precedes changes in apoptotic markers. Interestingly, Beclin-1 levels did not increase but decreased following 18 hour treatment.

We next identified the presence of autophagosomes by transmission electron microscopy (TEM). By TEM, we positively identified the presence of numerous double membrane autophagosomes with As_2O_3 treatment (Figure 3d and 3e). Following 3 hour As_2O_3 treatment, formation of double membrane structures was observed. At 9 hours, autophagosomes were fully formed and at 18 hours, clearing within autophagosomes appeared suggesting degradation of the cytoplasmic contents (Figure 3e). Beyond 18 hours, the cells underwent apoptosis (results not shown). In addition, we transfected EGFP-LC3 cDNA into HEY cells to identify fluorescent vacuoles following As_2O_3 treatment and observed a punctate staining pattern around the nucleus with 5μM to 25μM As_2O_3 compared to diffuse EGFP fluorescence in untreated cells (0μM As_2O_3) (see Figure 5a and 5b). Collectively, these results show that As_2O_3 induces the development of autophagosomes in parallel with induction of SnoN protein which precedes changes in apoptotic markers.

As_2O_3 mediates its effects in ovarian cells via the generation of reactive oxygen species (ROS)

To determine whether the As_2O_3–induced changes observed in expression of TGFβ signaling mediators are due to the effects of oxidative stress, we treated HEY cells with As_2O_3 in combination with the antioxidant N-acetyl-L-cysteine (NAC), a free radical scavenger/reducing agent and glutathione precursor which protects against As_2O_3-induced apoptosis in tumor cells.22 Light micrographs of cells co-treated with 10μM As_2O_3 and 1000μM NAC showed a dramatic reduction in cytoplasmic vacuolation and apoptotic morphology in contrast to cells treated with 10μM As_2O_3 alone (Figure 4a). Further, increasing doses of NAC markedly reduced SnoN with a corresponding recovery in EVI1

and TGFβRII proteins (Figure 4b, left panel). The results indicate that TGFβ signaling mediator expression can be altered by the presence of ROS. Although the levels of p62 remained unchanged or increased slightly, there was a reduction in LC3-I levels (Figure 4b, right panel). Further, we observed a dramatic reduction in punctate EGFP-LC3 staining suggesting As_2O_3-induced autophagy can be reversed by addition of antioxidant (Figure 4c, top and bottom panels). We observed an increase in cell survival following co-treatment with 10μM As_2O_3 and 1000μM NAC (Figure 4d) indicating that NAC promotes increased cellular viability. Since the level of cleaved PARP was difficult to detect at 10μM As_2O_3 (Figure 4b, right panel), we quantified changes in apoptosis by staining with annexin V-FITC and propidium iodide (PI) apoptosis. We observed a significant decrease in apoptotic cells upon co-treatment with 10μM As_2O_3 and NAC compared to As_2O_3-only treated cells (Figure 4e). Together, these results suggest that As_2O_3 mediates its effects via the generation of ROS which alters the autophagic and apoptotic response.

As_2O_3 induces autophagy via a Beclin-1 independent pathway

To determine whether autophagy is a necessary step in induction of cell death via As_2O_3, we tested the effects of various inhibitors of autophagy and apoptosis. 3-Methyladenine (3-MA) is a class III phosphatidylinositol-3-kinase (PI3K) inhibitor that inhibits autophagy at the earliest stage of autophagosome formation and is associated with decreased LC3-II expression.23 Although SnoN levels were not dramatically altered in HEY cells co-treated with As_2O_3 and 3-MA, there was reduced formation of EGFP-LC3 punctae (Figure 5a and 5b), decreased LC3 protein, and increased cleaved PARP (used as marker of apoptosis) in contrast to cells treated with 25μM As_2O_3 alone (Figure 5c). Although Beclin-1 levels were previously reported to be suppressed by 3-MA treatment,24 we did not detect any marked changes in Beclin-1 levels in HEY cells co-treated with 3-MA and As_2O_3 (Figure 5c). Moreover, addition of 3-MA to resveratrol treated ovarian cells failed to elicit a marked change in Beclin-1 or LC3 expression (Supplementary Figure 3a and 3b). In contrast, nutrient starvation with EBSS markedly increased both LC3 and Beclin-1 levels which were both reduced following treatment with 3-MA (Supplementary Figure 4a and 4b). We next investigated the effect of Bafilomycin A1 (BAF), a late-stage autophagy inhibitor that hinders fusion of lysosomes to autophagosomes leading to inhibition of the degradation of inner contents and accumulation of uncleaved LC3-II protein.25 Western analysis of HEY cells co-treated with As_2O_3 and Bafilomycin A1 showed increased LC3-II and cleaved PARP levels (Figure 5d, left panel). These results suggest that inhibition of late stage autophagy leads to increased apoptosis. Further, SnoN levels were slightly reduced with Bafilomycin A1 in the presence of As_2O_3 suggesting a role for SnoN in this process. In addition, we investigated the effect of zVAD-fmk, a caspase inhibitor which inhibits apoptosis, to provide additional evidence that As_2O_3-induced autophagy is independent of apoptosis.26 Although the levels of SnoN and LC3 remained unchanged with increasing concentrations of zVAD-fmk (Figure 5d, right panel), cleaved PARP was markedly reduced suggesting decreased apoptosis. Collectively, these results suggest that As_2O_3-induced autophagy confers a protective role against apoptosis which is the primary cell death mechanism induced by As_2O_3.

Since these inhibitors can induce non-specific effects, we thus assessed knockdown of specific ATG genes on autophagy and apoptosis in HEY cells. Several key regulators of autophagy were detectable by western analysis in ovarian cells such as hVps34, Beclin-1, ATG5, and ATG7 (Figure 5e). Although knockdown of Beclin-1 by siRNA treatment for 2 consecutive days effectively (>95%) reduced protein expression (Figure 5f), it did not affect expression of LC3-II/LC3-I (Figure 5f) or significantly modulate formation of LC3 punctae induced by As_2O_3 (Figure 5g and 5h). In contrast, ATG5, ATG7, and hVps34 siRNA markedly altered the ratio of LC3-II/LC3-I (Figure 5f) and LC3 punctae formation (Figure 5g and 5h). Staining with annexin V-FITC and propidium iodide (PI) showed only subtle changes in the apoptotic response with ATG siRNAs (Figure 5i). Furthermore, we assessed Beclin-1 knockdown with EBSS treatment which led to reduced LC3-II levels (Supplementary Figure 4c). However, we could not accurately assess the effect of EBSS on LC3 punctae formation due to the dramatically altered cell morphology (i.e. cell rounding). Together, these results suggest that As_2O_3 elicits its effects on autophagy in a Beclin-1 independent manner.

Modulation of the sensitivity of ovarian cancer cells to As_2O_3 by SnoN knockdown

Since we observed that SnoN levels paralleled those of LC3, we investigated whether SnoN could alter LC3-II levels and production of autophagosomes. Light microscopy suggests that knockdown of SnoN increases the sensitivity of the cells to As_2O_3 treatment leading to increased cell death compared to control siRNA treated cells (Figure 6a). In SnoN knockdown cells (>90% decrease in SnoN protein) treated with As_2O_3, western analysis showed a marked reduction in LC3-II and p62 levels with an increase in cleaved PARP compared to control siRNA cells treated with 25μM As_2O_3 (Figure 6b). These protein changes corresponded with a reduction in EGFP-LC3 punctae (Figure 6c), a marked reduction in cell survival (Figure 6d), and increased levels of apoptosis determined by annexin V-FITC and propidium iodide (PI) staining (Figure 6e). Thus, these data suggests that the sensitivity to As_2O_3–induced autophagy and apoptosis can be modulated by altering SnoN levels.

qPCR measurements of LC3 RNA transcripts indicated that its levels are low and SnoN siRNA did not modulate LC3 RNA transcripts (results not shown) suggesting alternative mechanisms other than direct transcriptional regulation of LC3 by SnoN. Since low and high expressing EVI1 ovarian cell lines differed in their response to the apoptotic effects of As_2O_3 (see Figure 2a and 2b), we assessed the effect of EVI1 siRNA on the sensitivity of ovarian cancer cells to As_2O_3. However, EVI1 siRNA (>90% reduction in wild type EVI1 protein) did not dramatically alter As_2O_3 induced sensitivity to apoptosis based on PARP cleavage levels or alter autophagy based on western analysis LC3-II levels (results not shown).

SnoN is reported to be degraded upon TGFβ stimulation by TAK1 via the ubiquitin-dependent proteosome pathway.14 Since we observed that As_2O_3 treatment decreased TAK1, we next assessed whether reducing TAK1 levels could alter As_2O_3-induced changes in SnoN and thus, modulate the autophagic pathway. However, TAK1 siRNA treatment (>80% knockdown) did not modulate SnoN levels, alter the sensitivity of ovarian cancer

cells to As_2O_3, or modulate p62 and LC3 protein levels (Figure 7a). However, knockdown of AKT, which lies downstream to PI3K27 and is a promising target for therapy in ovarian carcinomas,28,29 did not modulate expression of TGFβ signaling mediators, but did increase PARP cleavage while decreasing p62 levels and LC3-II/LC3-I levels (Figure 7b) suggesting that AKT plays a role in modulating the apoptotic and autophagic pathways.

Discussion

Since successful treatment of cancer cells with chemotherapeutic drugs is dependent on their ability to trigger cell death, it is critical to understand their mechanisms of action. Herein, we report that As_2O_3, commonly used to treat APL, can target TGFβ signaling mediators via proteosome-dependent (i.e. EVI1 and TGFβRII) and -independent pathways (SMAD2/3 and AKT) in ovarian cancer cell lines. The increased sensitivity of EVI1 forms to As_2O_3 following long-term treatments (18 hours) could be due to their inherent protein stability and long half-life. These As_2O_3 induced effects on EVI1 are similar to the reported effects in leukemia cell lines.10

In our studies, we observed different sensitivities to As_2O_3 among the three ovarian cell lines assessed (low (T80) and high (SKOV3 and HEY) expressing EVI1 ovarian cell lines) suggesting that the sensitivity of ovarian cell lines to As_2O_3 may correlate with EVI1 protein expression. However, knockdown of EVI1 (siRNA designed against Exon VII) failed to alter the sensitivity to As_2O_3 induced apoptosis. There are numerous other factors likely dictating cellular resistance or sensitivity to As_2O_3 including (1) GSH levels, (2) enzymes involved in biosynthesis of GSH, (3) enzymes using GSH (glutathione-S-transferase), (4) free radical scavenging and peroxide metabolism (GSH peroxidase, catalase), and (5) MRP1 levels which is involved in the efflux of As_2O_3 in drug-resistant cell lines. Indeed, we observed that MRP1 is highly expressed in both HEY and SKOV3 cells, which could result in resistance to As_2O_3.

As_2O_3 treatment dramatically elevated SnoN levels likely mediated through a ROS-dependent pathway (Figure 4b). As_2O_3 treatment can generate ROS, a form of oxidative stress, which can induce autophagy. Superoxide anion appears to be the major reactive oxygen species regulating autophagic process.30 Since ROS oxidizes cellular lipids, proteins, and DNA causing cellular damage, autophagy serves to prevent accumulation of these damaged toxic products and organelles by sequestering these cellular components into autophagosomes (double membraned vesicles) which fuse with lysosomes for degradation. Specifically, ROS can oxidize the cysteine protease, ATG4, involved in initiating the conjugation of LC3-I to autophagosomal membranes and its consequent release from the autophagophore membrane.31

We also observed that As_2O_3 treatment elevated SnoN levels in a TAK1-independent manner (Figure 7a). Interestingly, normal epithelial cells treated with TRAIL induced cytoprotective autophagy mediated via TAK1 which activates AMP-activated protein kinase leading to inhibition of mammalian target of rapamycin I.32 However, under our assay conditions, we failed to detect changes in autophagy or apoptosis upon depletion of TAK1 in HEY ovarian carcinoma cells (see Figure 7a).

Signaling pathways determining whether cells undergo autophagy or apoptosis are complex. In malignant glioma cells, As_2O_3 appears to initiate an autophagic response that leads to cell death.33 This contrasts to our data in ovarian cell lines based on inhibitor studies with 3-MA and zVAD-fmk suggesting cell-type specific effects of As_2O_3. Indeed, autophagy has been described as a “double edged sword” promoting (1) survival in response to stress and starvation as well as (2) programmed cell death.34 Recently, autophagy-related proteins such as Beclin-1 or ATG5/12 do not appear to be required for the autophagic process suggesting alternative non-canonical macroautophagy pathways.35,36 In our ovarian carcinoma cells, Beclin-1 appeared to be dispensable for inducing As_2O_3-mediated autophagic response but was dependent on hVps34.

SnoN protein not only paralleled the autophagy marker (LC3-II) but knockdown of SnoN altered LC3-II/I ratios suggesting that this protein lies downstream to SnoN. Other mediators important in As_2O_3-induced programmed cell death includes p21, which itself leads to cell cycle arrest and apoptosis.37 Indeed, we have previously shown that SnoN knockdown increases p21 protein levels.4 Thus, SnoN may play a key role in autophagy to promote cell survival as a protective mechanism against As_2O_3-induced cell death (Figure 8). The mechanism by which SnoN alters autophagosome development is presently under investigation.

Materials and Methods

Cell Lines and Cell Culture

The following ovarian cell lines were used for the studies reported herein: T antigen/hTERT immortalized normal ovarian surface epithelial cells (T80) as well as several ovarian carcinoma cell lines, including SKOV3 (amplification at the EVI1 locus), HEY (high expressing EVI1 cell line), and OVCA429 (high expressing EVI1 cell line).2 Cell lines were cultured in RPMI 1640 with 8% FBS and penicillin/streptomycin and maintained in an incubator with a humidified atmosphere containing 95% air and 5% CO_2 at 37°C. For nutrient starvation, cells were washed three times with Earle’s balanced salt solution (EBSS) (Invitrogen (Carlsbad, CA)) and then replaced with EBSS.

siRNA Treatment of Ovarian Cell Lines

The ovarian cancer cells, HEY and OVCA429, were plated at 250,000 cells (unless otherwise specified) in each well of a 6-well plate. The following day, the cells were transfected using 20μM siRNA against SnoN (Ambion (Austin, TX), ID#107696 or ID#107695), EVI1 Exon VII (Dharmacon (Lafayette, CO), custom-designed sequence: sense 5’ ACU ACG UCU UCC UUA AAU AUU-3’), AKT (Cell Signaling Technology (Danvers, MA)), TAK1 (Dharmacon, custom-designed sequence: sense 5’-GUA GAU CCA UCC AAG ACU UUU-3’), SMURF2 (Dharmacon, L-007194-00), ATG5 (Dhamarcon, L-004374-00), Beclin-1 (Dharmacon, L-010552-00), ATG7 (Dharmacon, L-020112-00), hVps34 (Applied Biosystems (Foster City, CA), ID#10517), or non-targeting control-1 siRNA (Dharmacon, D-001210-01) using Dharmafect I transfection reagent (Dharmacon). Briefly, cells were cultured in complete medium for 24 hours prior to transfection (2ml media in each well of 6-well plate) at which time the medium was changed to serum and

antibiotic-free medium. Dharmafect I (4μl) was incubated in 100μl of serum and antibiotic-free media for 10 minutes at room temperature, followed by the addition of 5μl of siRNA (20μM) and further incubated for 20 minutes at room temperature. The mixture was added to the cells and incubated for 48 hours prior to isolation of RNA and protein for qPCR and western analysis, respectively.

Cell Treatments with Clinical Inhibitors

The clinical inhibitors As_2O_3, MG132 (dissolved in DMSO) were obtained from Sigma-Aldrich (St. Louis, MO), Fisher Scientific (Pittsburg, PA), and Alexis Biochemicals (Farmingdale, NY), respectively. N-acetyl-L-cysteine (NAC; dissolved in media) and Bortezomib (PS-341; dissolved in DMSO) were obtained from Fisher Scientific. Resveratrol (dissolved in DMSO) was obtained from EMD Biosciences (Gibbstown, NJ). 3-Methyladenine (3-MA; dissolved in media) was obtained from MP Biomedicals (Solon, OH). zVAD-fmk (dissolved in DMSO) and Bafilomycin A1 (dissolved in DMSO) was obtained from Axxora LLC (San Diego, CA). Ovarian cells were plated in 6-well plates at 250,000 cells per well and grown in complete medium. The following day, the cells were treated with 5μM MG132, As_2O_3 (between 2–50μM), resveratrol (between 10–100μM), NAC (Fisher Scientific, between 25μM to 1mM), 3-MA (0.1mM to 10mM), or zVAD-fmk (25μM to 100μM). For detection of apoptosis by western analysis, it was generally difficult to detect cleaved PARP at 10μM As_2O_3 treatment but it was clearly observable with 25μM As_2O_3 (see Figure 3a). For functional assays (cell viability, apoptosis by PI/Annexin V staining, and EGFP-LC3 staining), we treated cells with 10μM As_2O_3 which allowed detection of differences more clearly with various treatments including siRNA knockdown (see Figure 2c). For control cells, DMSO (a final concentration of <0.5%) was added to compare appropriately to drugs dissolved in DMSO. After the appropriate incubation time (6 or 18 hours), cell lysates were collected, protein quantified, and SDS-PAGE/western analysis was performed. In addition, for selected studies, RNA was isolated, quantified, and used for qPCR analysis.

Quantitative PCR

RNA was isolated using the RNeasy Mini Kit (Qiagen, Valencia, CA). Quantitative PCR (qPCR) was performed using the one-step RT-PCR Taqman master mix from Applied Biosystems (Foster City, CA) with the following primers and probe sets.

EVI1 Exon III - (detects both EVI1 and MDS1/EVI1):

Forward primer, CGAAGACTATCCCCATGAAACTATG;

Reverse primer, TCACAGTCTTCGCAGCGATATT;

Probe sequence, TCCACGAAGACGGA.

Primers/probe sequences for SnoN (Hs00180524_m1), TGFβRII (Hs00234253_m1), and LC3 (Hs00261291_m1) were obtained from Applied Biosystems (Assays by Design). mRNA levels were determined using the One-Step-Plus Applied Biosystems Detection System using β-actin as a reference. PCR conditions were as follows: stage I: 48°C for 30 min; stage II: 95°C for 10 min; stage III: [40 cycles] 95°C for 15 s followed by 60°C for 1 min. Using the correlative method, RNA-fold change in expression was calculated as Ct of

gene – Ct of β-actin to generate delta Ct from which delta Ct of the normal sample was subtracted. These values were then converted to $\log_2$ values.

SDS-PAGE and Western Blot Analyses

Proteins were resolved on an 8%, 12%, or 15% SDS-PAGE gel (as appropriate) and electrophoretically transferred to polyvinyldifluoride (PVDF) membranes. After blocking with 5% (w/v) milk in TBST (Tris-Buffered Saline containing 0.1%Tween-20) for one hour at room temperature, membranes were incubated with primary antibodies (at appropriate dilution) overnight at 4°C, followed by extensive washing and incubation for 1 hour with the appropriate horseradish peroxidase-conjugated secondary antibodies (BioRad, Hercules, CA). Blots were washed extensively and developed using chemiluminescence substrate (BioRad). A rabbit polyclonal EVI1 antibody was obtained from Dr. J. Ihle (1:3000 dilution, St. Jude's Children's Hospital, Memphis, TN). SnoN rabbit polyclonal (1:1000 dilution), SMURF2 rabbit polyclonal (1:500 dilution), MRP1 mouse monoclonal (1:500 dilution) and GAPDH mouse monoclonal (1:250 dilution) antibodies were obtained from Santa Cruz Biotechnology (Santa Cruz, CA). TGFβRII rabbit polyclonal (1:1000 dilution) antibody was obtained from Strategic Diagnostics (Newark, DE). SMAD2/3 rabbit polyclonal (1:1000 dilution), AKT rabbit polyclonal (1:1000 dilution), TAK1 rabbit polyclonal (1:1000 dilution), PARP rabbit polyclonal (1:1000 dilution), Beclin-1 rabbit polyclonal (1:1000 dilution), caspase-3 rabbit polyclonal (1:1000) which detects the pro-caspase form, ATG5 rabbit polyclonal (1:1000 dilution), hVps34 rabbit polyclonal (1:1000 dilution), LC3 rabbit polyclonal (1:1000 dilution) antibodies were obtained from Cell Signaling Technology (Danvers, MA). The p62 Dok mouse monoclonal (1:1000 dilution) antibody was obtained from BD Biosciences (San Jose, California). The ATG7 rabbit polyclonal (1:1000 dilution) antibody was obtained from MBL International (Woburn, MA).

Densitometric analysis was performed using the Hp Scanjet 5590 and the Image J program (Image Processing and Analysis in Java, NIH Image Software). Bands were selected and the intensity values were normalized to those for GAPDH. The values are presented as fold-changes relative to control siRNA treated cells.

Migration Assays

Immortalized normal ovarian epithelial cells (T80) and ovarian cancer cells (SKOV3 and HEY) were treated with 5μM As_2O_3 for 6 hours. 25,000 cells were seeded into each Boyden chamber insert. After 18 hours, the cells were fixed and stained with crystal violet. The cells that migrated through the pores were counted using an inverted light microscope.

Cell Viability Assay Via Measurement of Intracellular ATP Levels

T80, HEY, and SKOV3 ovarian cells were seeded in triplicate for each treatment group at 5,000 cells per well into each well of a 96-well white-opaque plate. Following overnight cell attachment, cells were treated for 18 hours with appropriate doses of As_2O_3 (2μM, 5μM, 10μM, 25μM, and 50μM). Following termination of the cell treatments, the media was removed from the wells and replaced with 100μl of phosphate-buffered saline (PBS). The plate was equilibrated to room temperature, 100μl of CellTiter-Glo reagent (Promega, Madison, WI) was added, and mixed on a plate shaker for 2 minutes. The plate was further

incubated for 10 minutes at room temperature prior to reading with a Biotek luminescence plate reader to obtain relative light unit (RLU) measurements. Empty wells (containing no cells) were utilized as a correction for background luminescence. All experiments were performed in triplicate.

Apoptosis Assays

For assessment of apoptosis, the Annexin V-propidium iodide staining kit (Calbiochem, San Diego, CA) was used according to the manufacturer's protocol. Briefly, cells were treated with As_2O_3 for 24 hours at which time both the floating and adherent cells (removed by trypsinization) were collected. Cells were resuspended in PBS followed by the addition of annexin V-FITC and propidium iodide. The samples were then analyzed by flow cytometry at the MD Anderson Cancer Center and University of South Florida Health – College of Medicine FACS Core Facility. The FITC and the propidium iodide signals were detected at 518nm with FL1 and at 620nm with FL2, respectively. The log fluorescence values of annexin V-FITC and propidium iodide are displayed on the X and Y axis, respectively.

Electron Microscopy

To demonstrate the induction of autophagy in arsenic trioxide treated cells morphologically, HEY cells were treated with or without As_2O_3 (dose) across a series of time points (h) in T-75 culture flasks. Cells were then fixed in 2.5% glutaraldehyde in 0.1M phosphate buffer overnight at 4°C. Following rinsing in buffer, cells were scraped from the culture flasks, washed, and then post-fixed in 1% osmium tetroxide in buffer. After dehydration in a graded series of acetone, the cells were embedded in Embed 812 epoxy resin. Thin sections (70nm) were cut on an Ultramicrotome. The sections on the grids were stained with uranyl acetate and lead citrate. The sections were examined on a Transmission Electron Microscope (Morgagni 268D).

Indirect Immunofluorescence

HEY cells were seeded onto glass coverslips and allowed to adhere following overnight incubation. The cells were then transiently transfected with EGFP-LC3 (Addgene, Cambridge, MA) and allowed to recover for 24 hours. The cells were treated at the appropriate concentrations of As_2O_3 in the absence or presence of 3-MA (5 and 10mM) for 18 hours. The cells were then fixed in 4% formaldehyde in PBS for 30 minutes at room temperature, washed twice in PBS, and blocked for 1 hour at room temperature in PBS containing 5% goat serum and 0.1% Triton X-100. The cells were washed 3 times for 5 minutes in PBS, anti-Fade containing DAPI nuclear stain was then applied, coverslips mounted onto glass slides and viewed under a Zeiss inverted fluorescence microscope (Moffitt Cancer Center Microscopy Core). Quantification of EGFP-LC3 expressing cells was assessed by counting the number of cells containing punctate dots in a total of 200 EGFP-LC3 positive cells.

For indirect immunofluorescence of endogenous LC3B expression, HEY cells fixed in 4% formaldehyde in phosphate-buffered saline (PBS) for 30 minutes at room temperature, washed twice in PBS, and blocked for 1 hour at room temperature in PBS containing 5% goat serum and 0.1% Triton X-100. Primary antibodies (LC3B used at 1:2000 dilution) were

incubated in PBS containing 1% goat serum and 0.1% Triton X-100 overnight at 4°C. The cells were washed 3 times for 5 minutes in PBS and then incubate with the appropriate cy3-fluorescent conjugated rabbit antibody for 1 hour in PBS containing 1% goat serum and 0.1% Triton X-100. The cells were washed 3 times for 5 minutes in PBS, anti-Fade containing DAPI nuclear stain was then applied, coverslips mounted onto glass slides, and viewed under a fluorescence microscope.

Glutathione Measurement Assays

Glutathione (GSH) was measured using the GSH-Glo kit (Promega). Briefly, T80, HEY, and SKOV3 ovarian cells were plated at 5000 cells/well in opaque white 96-well plates. Following overnight attachment, cells were treated with As_2O_3 for 18 hours. Following cell treatments, the media was discarded and fresh PBS was added for washout followed by the addition of 100μl of GSH-Glo reagent. Following a 2 minute shake, the cells were incubated at room temperature for 30 minutes followed by the addition of reconstituted luciferase detection reagent. The cells were incubated for a further 15 minutes at room temperature and the plate was read on a Biotek luminescence plate reader. All measurements were performed in triplicate.

Statistical Analyses

Values are reported as the mean +/− standard deviation (S.D.) of independent experiments (see Figure Legends). In cell viability assays, the data are normalized to control cells and expressed as the percentage of live cells relative to total cells.

Supplementary Material

Refer to Web version on PubMed Central for supplementary material.

Acknowledgements

This work was supported by RO1 CA123219 to GBM and MN. This work has been supported in part by the Flow Cytometry Core Facility at the MD Anderson Cancer Center and University of South Florida. We gratefully acknowledge Dr. Kenyon Daniel for discussion and critical reading of the manuscript. We also kindly acknowledge Mitchel Ruzek, Deena Whaba, Christie Campla, and Kyle Bauckman for their assistance on the studies reported herein.

References

1. Elliott RL, Blobe GC. Role of transforming growth factor Beta in human cancer. J Clin Oncol. 2005 Mar 20; 23(9):2078–2093. [PubMed: 15774796]
2. Nanjundan M, Nakayama Y, Cheng KW, Lahad J, Liu J, Lu K, et al. Amplification of MDS1/EVI1 and EVI1, located in the 3q26.2 amplicon, is associated with favorable patient prognosis in ovarian cancer. Cancer Res. 2007 Apr 1; 67(7):3074–3084. [PubMed: 17409414]
3. Sunde JS, Donninger H, Wu K, Johnson ME, Pestell RG, Rose GS, et al. Expression Profiling Identifies Altered Expression of Genes That Contribute to the Inhibition of Transforming Growth Factor-{beta} Signaling in Ovarian Cancer. Cancer Res. 2006 Sep 1; 66(17):8404–8412. [PubMed: 16951150]
4. Nanjundan MCK, Zhang F, Lahad J, Kuo WL, Schmandt R, Smith-McCune K, Fishman D, Gray JW, Mills GB. Overexpression of SnoN/SkiL, amplified at the 3q26.2 locus, in ovarian cancers: A role in ovarian pathogenesis. Molecular Oncology. 2007; 2(2)

5. Zhang TD, Chen GQ, Wang ZG, Wang ZY, Chen SJ, Chen Z. Arsenic trioxide, a therapeutic agent for APL. Oncogene. 2001 Oct 29; 20(49):7146–7153. [PubMed: 11704843]
6. Bornstein J, Sagi S, Haj A, Harroch J, Fares F. Arsenic Trioxide inhibits the growth of human ovarian carcinoma cell line. Gynecol Oncol. 2005 Dec; 99(3):726–729. [PubMed: 16243384]
7. Kong B, Huang S, Wang W, Ma D, Qu X, Jiang J, et al. Arsenic trioxide induces apoptosis in cisplatin-sensitive and -resistant ovarian cancer cell lines. Int J Gynecol Cancer. 2005 Sep-Oct; 15(5):872–877. [PubMed: 16174238]
8. Uslu R, Sanli UA, Sezgin C, Karabulut B, Terzioglu E, Omay SB, et al. Arsenic trioxide-mediated cytotoxicity and apoptosis in prostate and ovarian carcinoma cell lines. Clin Cancer Res. 2000 Dec; 6(12):4957–4964. [PubMed: 11156257]
9. Zhang J, Wang B. Arsenic trioxide (As(2)O(3)) inhibits peritoneal invasion of ovarian carcinoma cells in vitro and in vivo. Gynecol Oncol. 2006 Oct; 103(1):199–206. [PubMed: 16624393]
10. Shackelford D, Kenific C, Blusztajn A, Waxman S, Ren R. Targeted degradation of the AML1/MDS1/EVI1 oncoprotein by arsenic trioxide. Cancer Res. 2006 Dec 1; 66(23):11360–11369. [PubMed: 17145882]
11. Fears S, Mathieu C, Zeleznik-Le N, Huang S, Rowley JD, Nucifora G. Intergenic splicing of MDS1 and EVI1 occurs in normal tissues as well as in myeloid leukemia and produces a new member of the PR domain family. Proc Natl Acad Sci U S A. 1996 Feb 20; 93(4):1642–1647. [PubMed: 8643684]
12. Kilbey A, Bartholomew C. Evi-1 ZF1 DNA binding activity and a second distinct transcriptional repressor region are both required for optimal transformation of Rat1 fibroblasts. Oncogene. 1998 Apr 30; 16(17):2287–2291. [PubMed: 9619838]
13. Morishita K, Parganas E, Douglass EC, Ihle JN. Unique expression of the human Evi-1 gene in an endometrial carcinoma cell line: sequence of cDNAs and structure of alternatively spliced transcripts. Oncogene. 1990 Jul; 5(7):963–971. [PubMed: 2115646]
14. Kajino T, Omori E, Ishii S, Matsumoto K, Ninomiya-Tsuji J. TAK1 MAPK kinase kinase mediates transforming growth factor-beta signaling by targeting SnoN oncoprotein for degradation. J Biol Chem. 2007 Mar 30; 282(13):9475–9481. [PubMed: 17276978]
15. Conery AR, Cao Y, Thompson EA, Townsend CM Jr, Ko TC, Luo K. Akt interacts directly with Smad3 to regulate the sensitivity to TGF-beta induced apoptosis. Nat Cell Biol. 2004 Apr; 6(4): 366–372. [PubMed: 15104092]
16. Wrighton KH, Lin X, Feng XH. Critical regulation of TGFbeta signaling by Hsp90. Proc Natl Acad Sci U S A. 2008 Jul 8; 105(27):9244–9249. [PubMed: 18591668]
17. Cheng B, Yang X, Han Z, An L, Liu S. Arsenic trioxide induced the apoptosis of laryngeal cancer via down-regulation of survivin mRNA. Auris, nasus, larynx. 2008 Mar; 35(1):95–101. [PubMed: 17869043]
18. Wu X, Chen Z, Liu Z, Zhou H, You Y, Li W, et al. Arsenic trioxide inhibits proliferation in K562 cells by changing cell cycle and survivin expression. Journal of Huazhong University of Science and Technology Medical sciences. 2004; 24(4):342–344. 353.
19. Davison K, Cote S, Mader S, Miller WH. Glutathione depletion overcomes resistance to arsenic trioxide in arsenic-resistant cell lines. Leukemia. 2003 May; 17(5):931–940. [PubMed: 12750708]
20. Salerno M, Petroutsa M, Garnier-Suillerot A. The MRP1-mediated effluxes of arsenic and antimony do not require arsenic-glutathione and antimony-glutathione complex formation. J Bioenerg Biomembr. 2002 Apr; 34(2):135–145. [PubMed: 12018890]
21. Bjorkoy G, Lamark T, Johansen T. p62/SQSTM1: a missing link between protein aggregates and the autophagy machinery. Autophagy. 2006 Apr-Jun;2(2):138–139. [PubMed: 16874037]
22. Han YH, Kim SZ, Kim SH, Park WH. Suppression of arsenic trioxide-induced apoptosis in HeLa cells by N-acetylcysteine. Molecules and cells. 2008 Jul 31; 26(1):18–25. [PubMed: 18511884]
23. Hoang B, Benavides A, Shi Y, Frost P, Lichtenstein A. Effect of autophagy on multiple myeloma cell viability. Mol Cancer Ther. 2009 Jul; 8(7):1974–1984. [PubMed: 19509276]
24. Qian W, Liu J, Jin J, Ni W, Xu W. Arsenic trioxide induces not only apoptosis but also autophagic cell death in leukemia cell lines via up-regulation of Beclin-1. Leuk Res. 2007 Mar; 31(3):329–339. [PubMed: 16882451]

25. Wu YC, Wu WK, Li Y, Yu L, Li ZJ, Wong CC, et al. Inhibition of macroautophagy by bafilomycin A1 lowers proliferation and induces apoptosis in colon cancer cells. Biochem Biophys Res Commun. 2009 May 1; 382(2):451–456. [PubMed: 19289106]
26. White E. Autophagic cell death unraveled: Pharmacological inhibition of apoptosis and autophagy enables necrosis. Autophagy. 2008 May 16; 4(4):399–401. [PubMed: 18367872]
27. Bellacosa A, de Feo D, Godwin AK, Bell DW, Cheng JQ, Altomare DA, et al. Molecular alterations of the AKT2 oncogene in ovarian and breast carcinomas. Int J Cancer. 1995 Aug 22; 64(4):280–285. [PubMed: 7657393]
28. Shayesteh L, Lu Y, Kuo WL, Baldocchi R, Godfrey T, Collins C, et al. PIK3CA is implicated as an oncogene in ovarian cancer. Nat Genet. 1999 Jan; 21(1):99–102. [PubMed: 9916799]
29. Meng Q, Xia C, Fang J, Rojanasakul Y, Jiang BH. Role of PI3K and AKT specific isoforms in ovarian cancer cell migration, invasion and proliferation through the p70S6K1 pathway. Cell Signal. 2006 Dec; 18(12):2262–2271. [PubMed: 16839745]
30. Chen Y, Azad MB, Gibson SB. Superoxide is the major reactive oxygen species regulating autophagy. Cell death and differentiation. 2009 Jul; 16(7):1040–1052. [PubMed: 19407826]
31. Scherz-Shouval R, Shvets E, Elazar Z. Oxidation as a post-translational modification that regulates autophagy. Autophagy. 2007 Jul-Aug;3(4):371–373. [PubMed: 17438362]
32. Herrero-Martin G, Hoyer-Hansen M, Garcia-Garcia C, Fumarola C, Farkas T, Lopez-Rivas A, et al. TAK1 activates AMPK-dependent cytoprotective autophagy in TRAIL-treated epithelial cells. Embo J. 2009 Mar 18; 28(6):677–685. [PubMed: 19197243]
33. Kanzawa T, Kondo Y, Ito H, Kondo S, Germano I. Induction of autophagic cell death in malignant glioma cells by arsenic trioxide. Cancer Res. 2003 May 1; 63(9):2103–2108. [PubMed: 12727826]
34. Rubinsztein DC, Cuervo AM, Ravikumar B, Sarkar S, Korolchuk V, Kaushik S, et al. In search of an "autophagomometer". Autophagy. 2009 Jul; 5(5):585–589. [PubMed: 19411822]
35. Scarlatti F, Maffei R, Beau I, Codogno P, Ghidoni R. Role of non-canonical Beclin 1-independent autophagy in cell death induced by resveratrol in human breast cancer cells. Cell death and differentiation. 2008 Aug; 15(8):1318–1329. [PubMed: 18421301]
36. Nishida Y, Arakawa S, Fujitani K, Yamaguchi H, Mizuta T, Kanaseki T, et al. Discovery of Atg5/Atg7-independent alternative macroautophagy. Nature. 2009 Oct 1; 461(7264):654–658. [PubMed: 19794493]
37. Liu ZM, Huang HS. Inhibitory role of TGIF in the As2O3-regulated p21 WAF1/CIP1 expression. Journal of biomedical science. 2008 May; 15(3):333–342. [PubMed: 18210215]

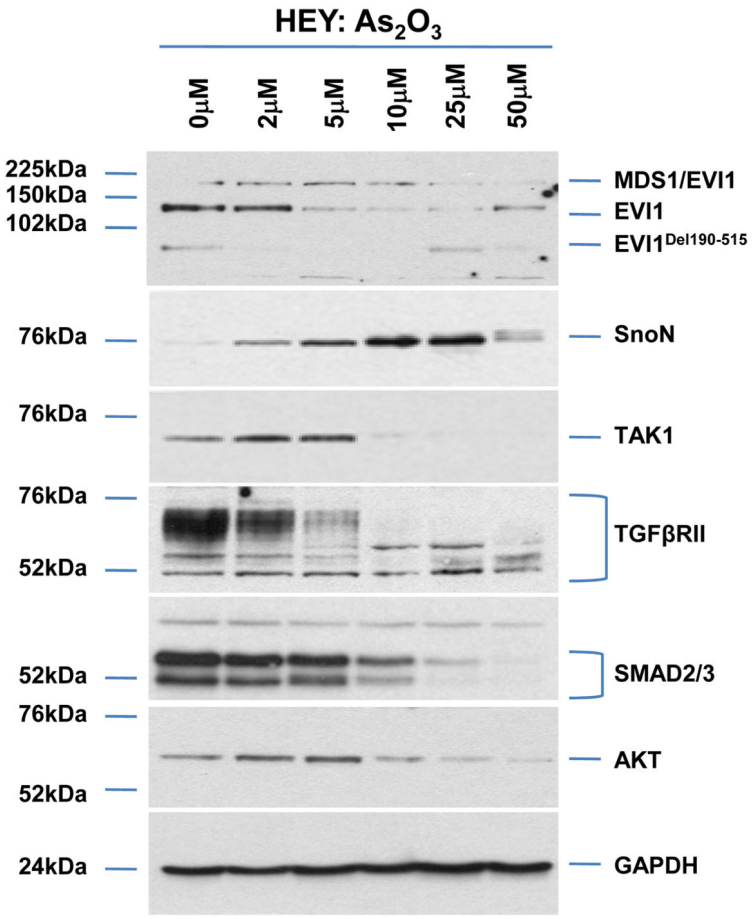

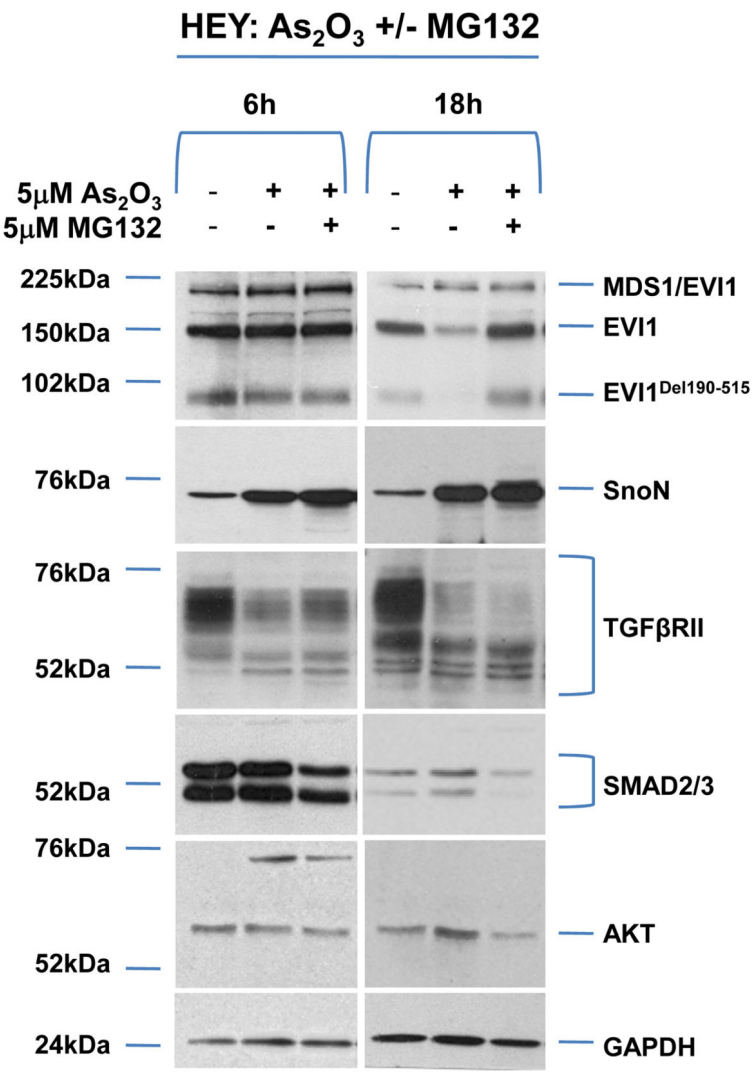

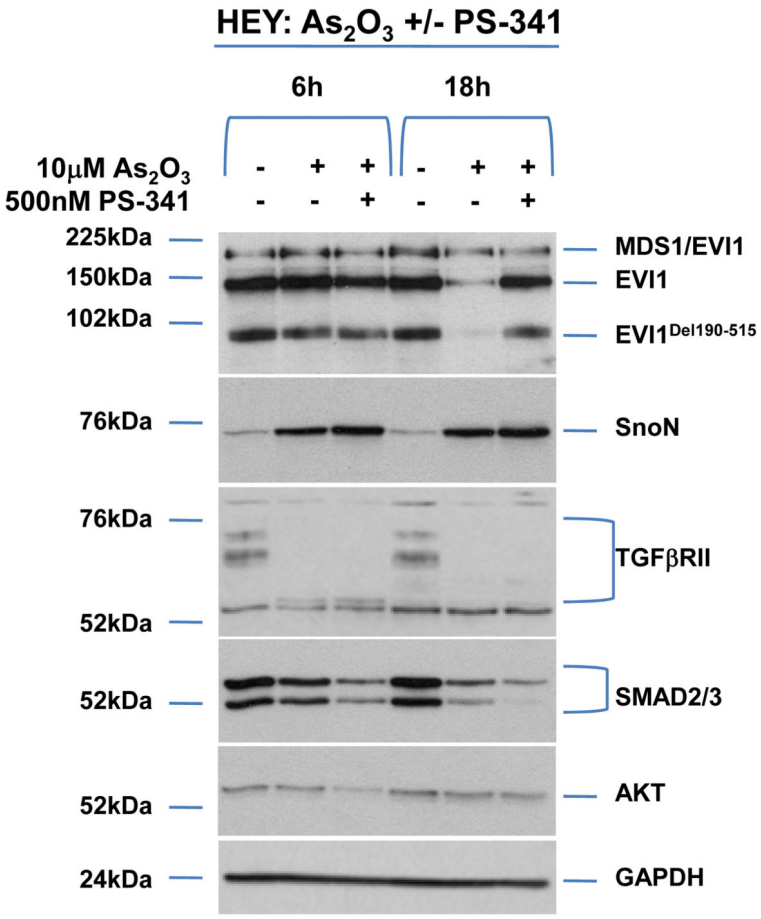

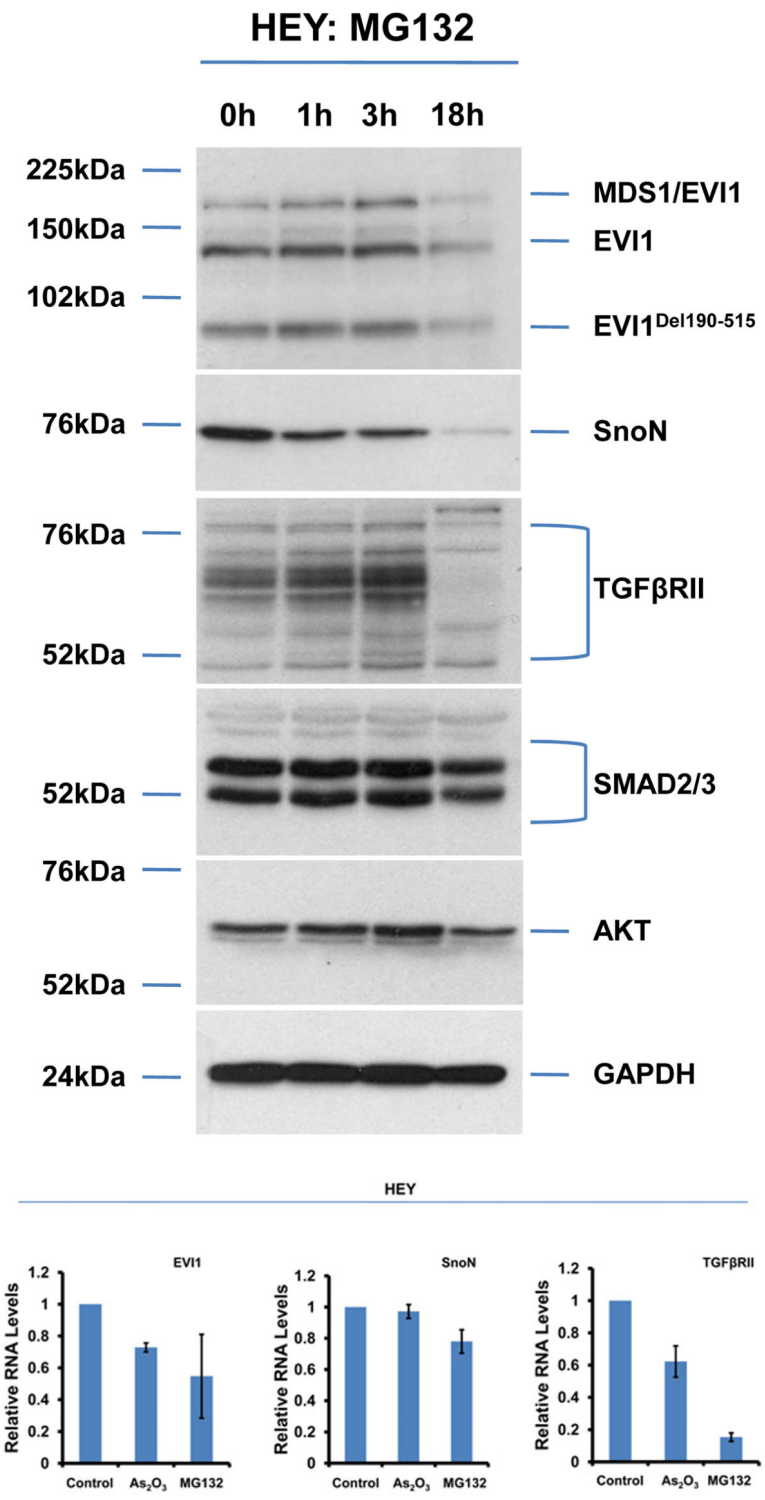

Figure 1.

As_2O_3 alters expression of TGFβ signaling mediators in HEY ovarian cancer cell line. **(a)** HEY cells were seeded at 250,000 cells per well in 6-well plates. After overnight attachment, the cells were treated with varying concentrations of As_2O_3 (2–50μM). After 18

hour incubation, the cell lysates were harvested and western analysis was performed using the following antibodies: (1) EVI1, (2) SnoN, (3) TAK1, (4) TGFβRII, (5) SMAD2/3, (6) AKT, and (7) GAPDH as a loading control. The data shown are representative of 4 independent experiments. **(b)** HEY cells were seeded at 250,000 cells per well in 6-well plates. After overnight attachment, the cells were treated with (1) 5μM As_2O_3, (2) 5μM MG132, or (3) 5μM As_2O_3 and 5μM MG132. After 6 or 18 hour treatment, the cell lysates were harvested and western analysis was performed using the following antibodies: (1) EVI1, (2) SnoN, (3) TGFβRII, (4) SMAD2/3, (5) AKT, and (6) GAPDH as a loading control. The data shown are representative of 3 independent experiments. **(c)** HEY cells were seeded at 250,000 cells in 6-well plates. After overnight attachment, the cells were treated with (1) 10μM As_2O_3, (2) 500nM PS-341, or (3) 10μM As_2O_3 and 500nM PS-341. After 18 hour treatment, the cell lysates were harvested and western analysis was performed using the following antibodies: (1) EVI1, (2) SnoN, (3) TGFβRII, (4) SMAD2/3, (5) AKT, and (6) GAPDH as a loading control. The data shown are representative of 3 independent experiments. **(d)** HEY cells were seeded at 250,000 cells per well in 6-well plates. After 24 hours, the cells were treated at different time points (1, 3, 18h) with 5μM MG132. Cell lysates were harvested and western analysis was performed using the following antibodies: (1) EVI1, (2) SnoN, (3) TGFβRII, (4) SMAD2/3, (5) AKT, and (6) GAPDH as a loading control. The data shown are representative of 3 independent experiments. **(e)** HEY cells were seeded at 500,000 cells per well in 6-well plates. Following 24 hours, the cells were treated with (1) DMSO, (2) 5μM As_2O_3 and DMSO, or (3) 5μM MG132 for 18 hours. RNA was then isolated and used for qPCR. Relative RNA-fold changes are presented for EVI1, SnoN, and TGFβRII. The data shown are representative of 3 independent experiments.

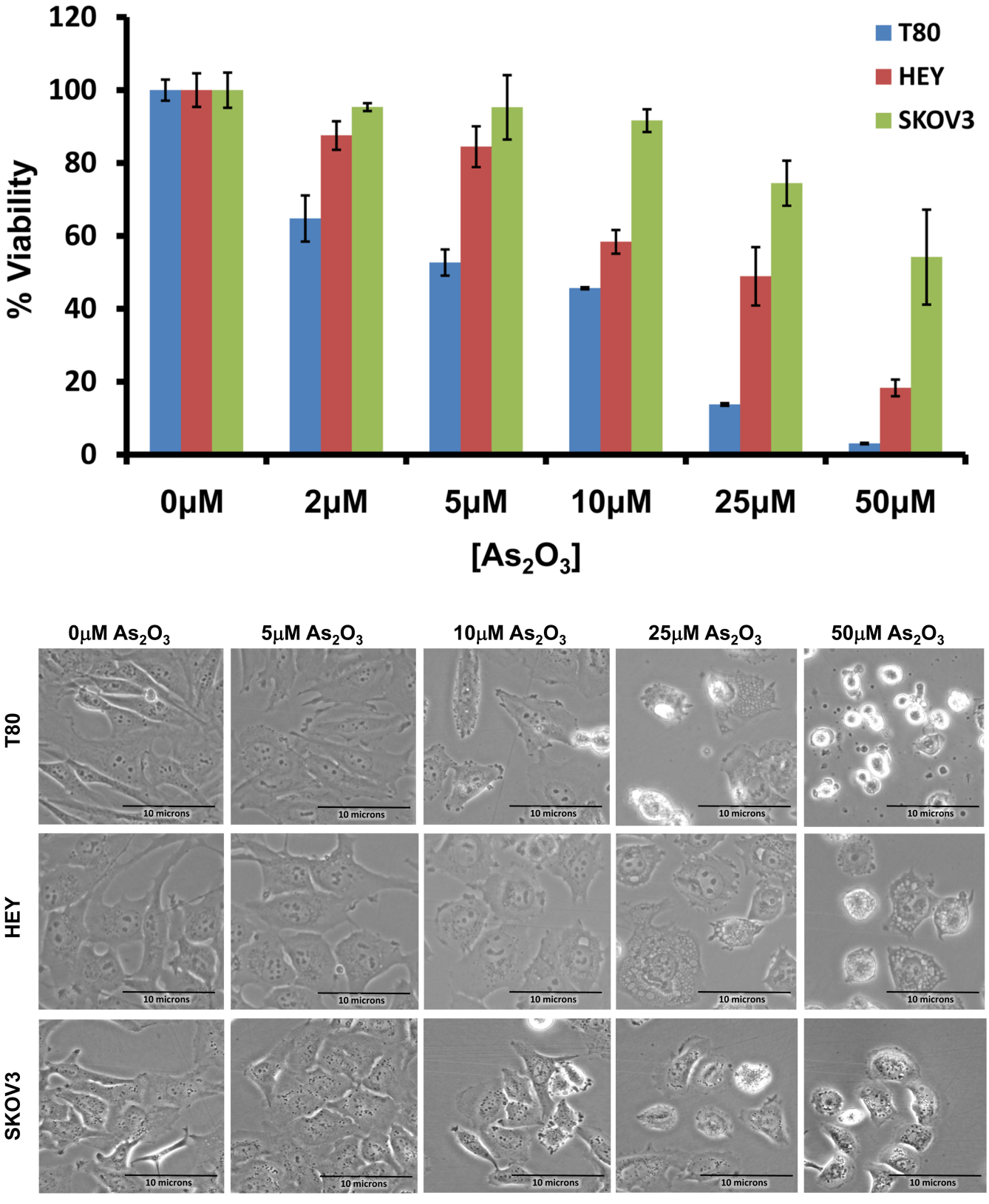

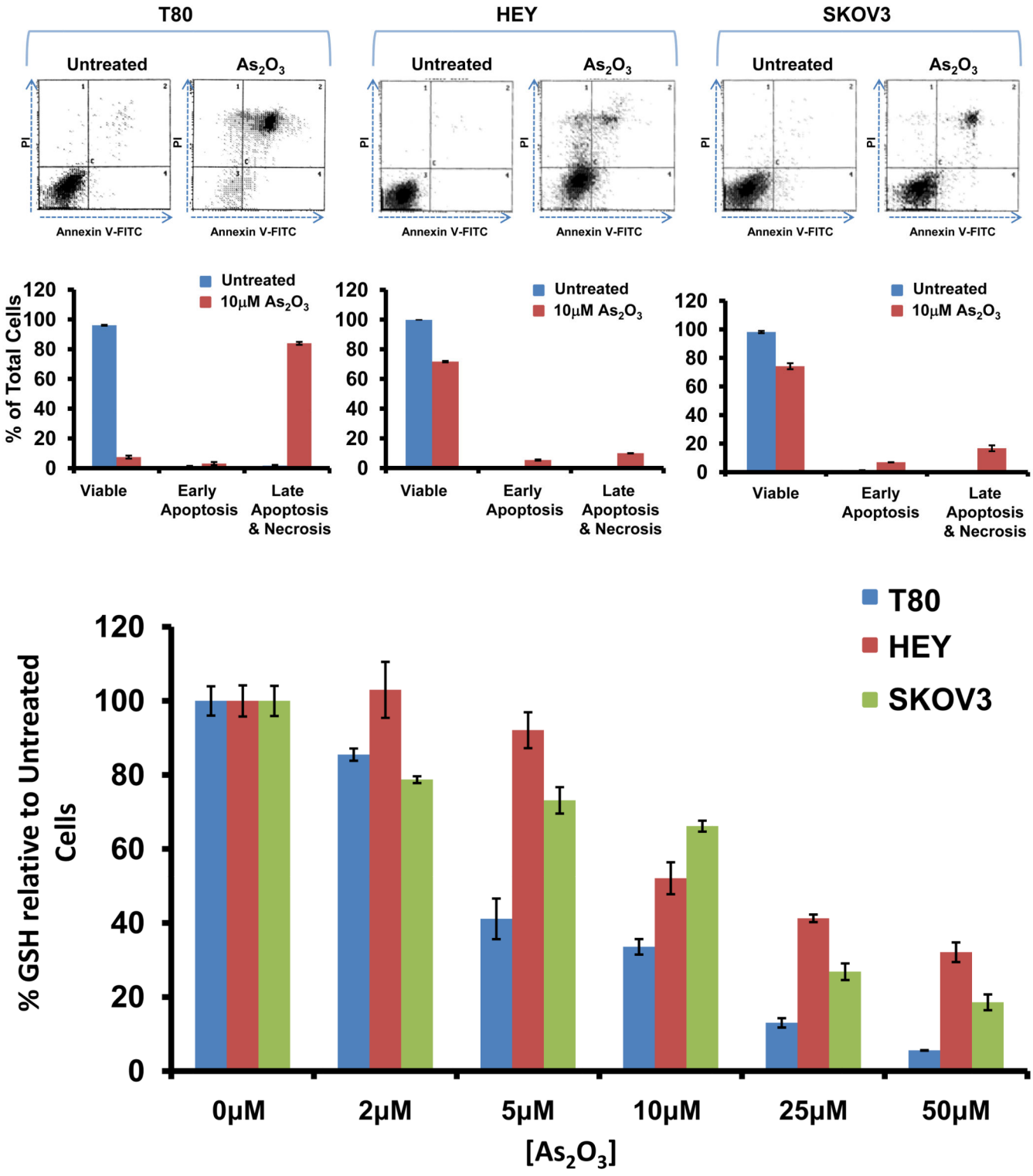

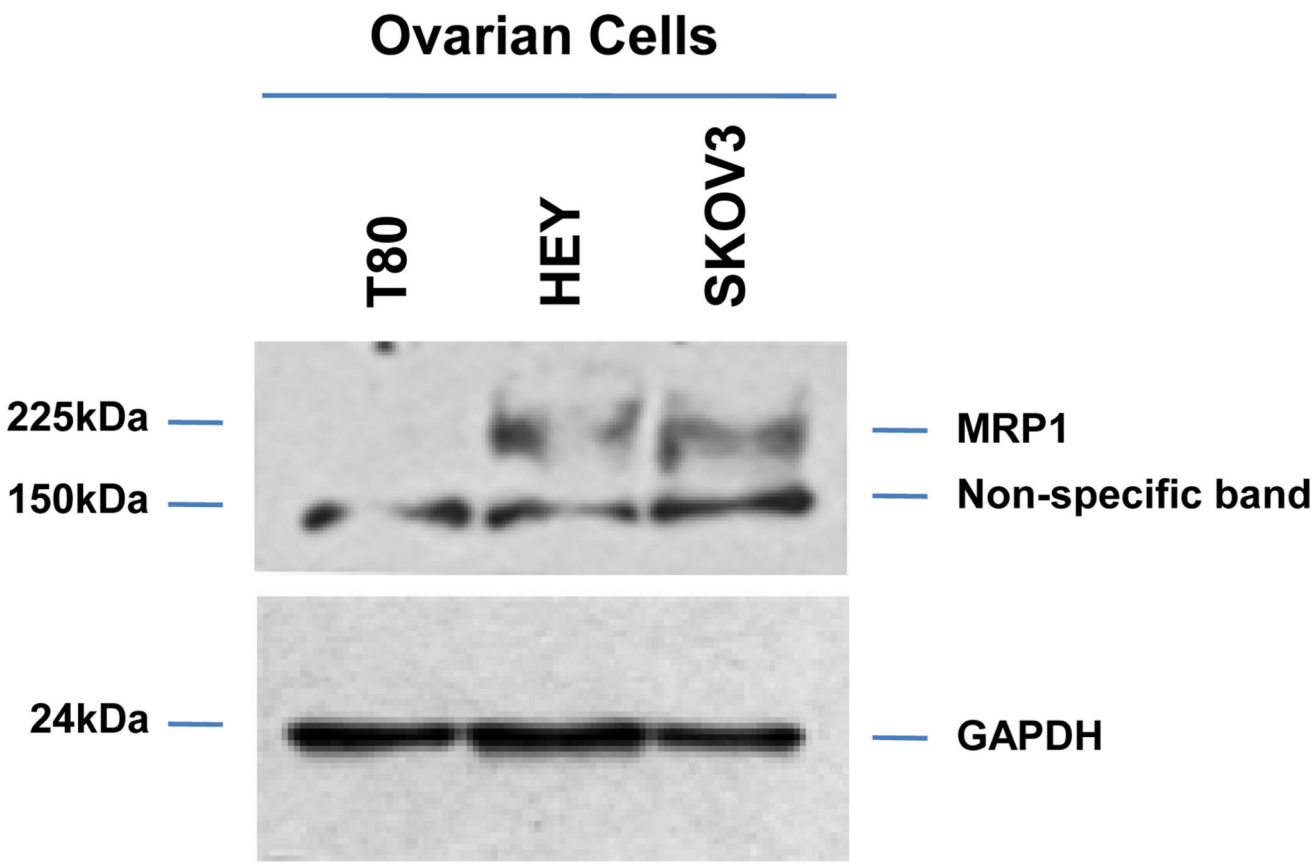

Figure 2.

As_2O_3 induces cell death. **(a)** Cell viability was assessed using the CellTiter-Glo assay in T80, HEY, and SKOV3 cells treated for 18 hours with varying doses of As_2O_3 (2–50μM). Results are presented as % cell viability relative to control cells (0μM). The data shown are representative of 3 independent experiments. **(b)** T80, HEY, and SKOV3 cells were seeded at 250,000 cells per well. After 24 hours, the cells were treated with varying concentrations of As_2O_3 (5–50μM). Following 18 hour treatment, images were captured at 40× magnification. The data shown are representative images. **(c)** HEY cells were seeded at 250,000 cells per well in 6-well plates. Following cell attachment, cells were treated with 10μM As_2O_3 at which time both the floating and adherent cells were collected. Cells were stained with annexin V-FITC and propidium iodide (PI) followed by flow cytometric analysis. (Top panels) Raw data plots are shown as log fluorescence values of annexin V-FITC and PI on the X and Y axis, respectively. (Bottom panels) The data is displayed in bar graphs as the percentage of viable, early apoptotic, and late apoptotic/necrotic cells. The data shown are representative of 2 independent experiments. **(d)** GSH levels were quantified in T80, HEY, and SKOV3 cells using the GSH-glo assay kit. Results are presented as % GSH relative to untreated cells. The data shown are representative of 3 independent experiments. **(e)** T80, HEY, and SKOV3 cells were grown to confluence in T-25 flasks. Cell lysates were harvested into 200μl of lysis buffer containing 10mM sodium orthovanadate, 100mM sodium fluoride, and protease cocktail inhibitors. Western analysis was performed

using the following antibodies: (1) MRP1 and (2) GAPDH. The data are representative of 2 independent experiments.

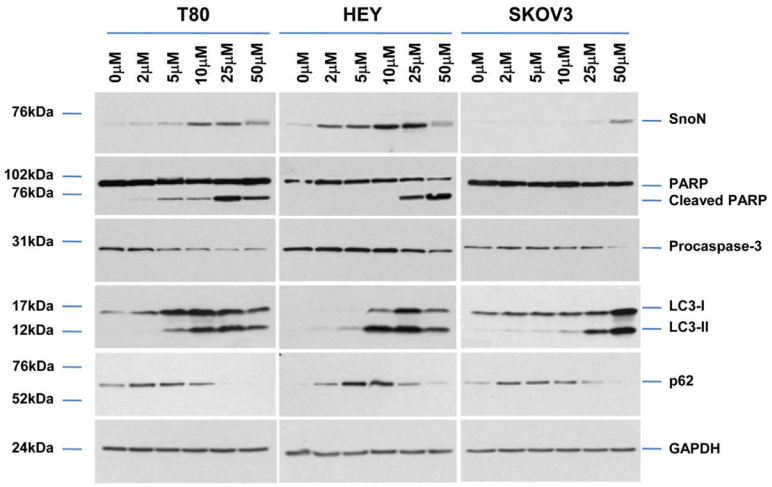

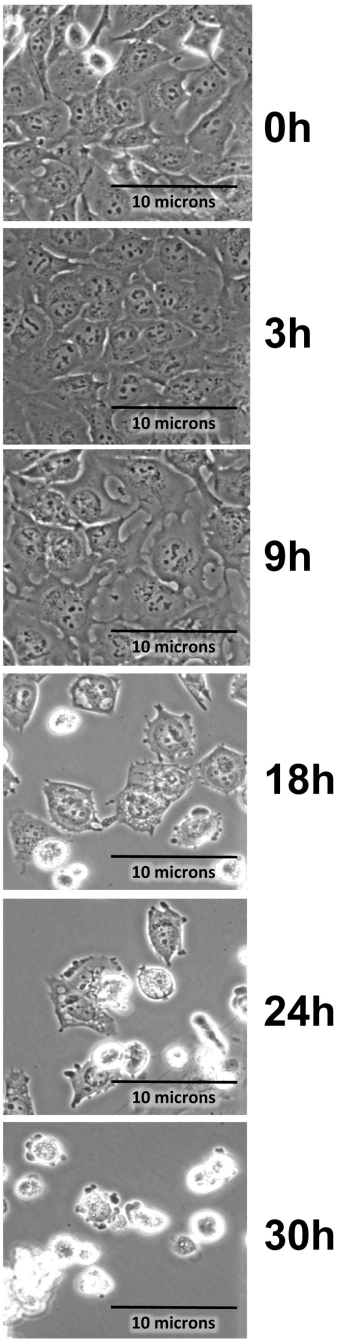

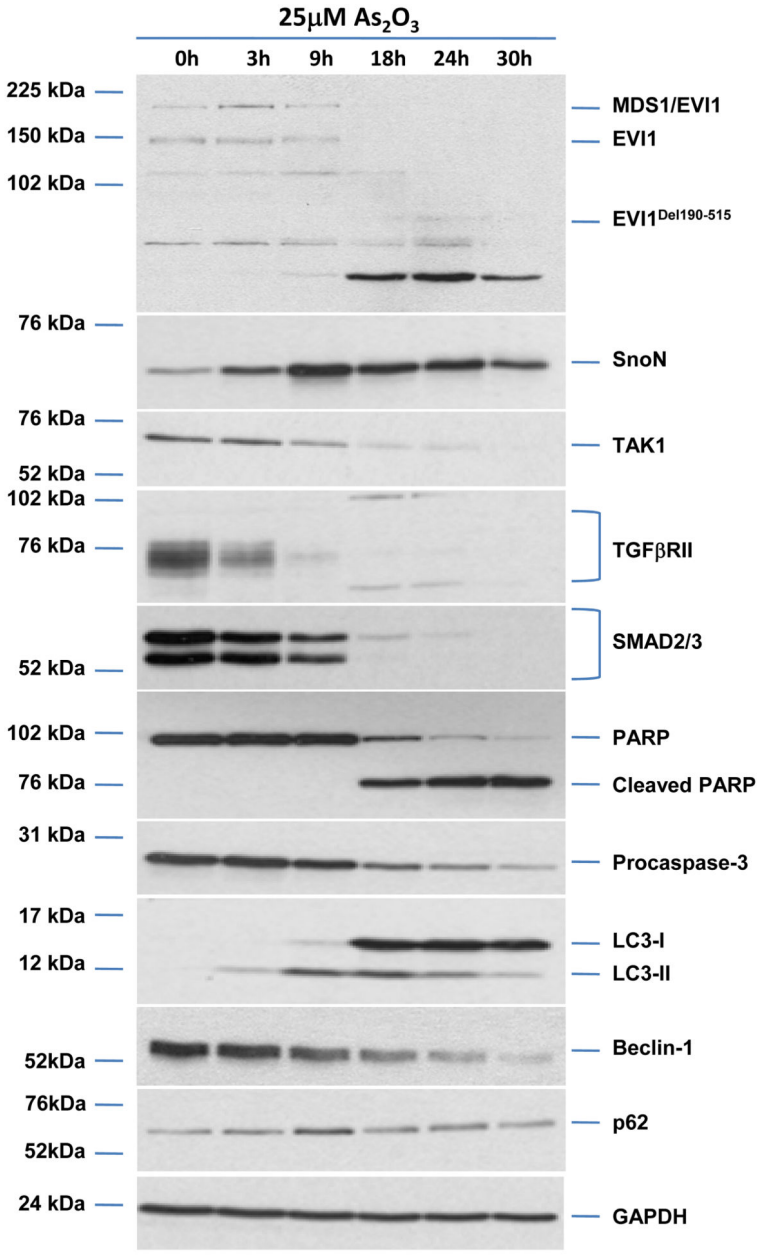

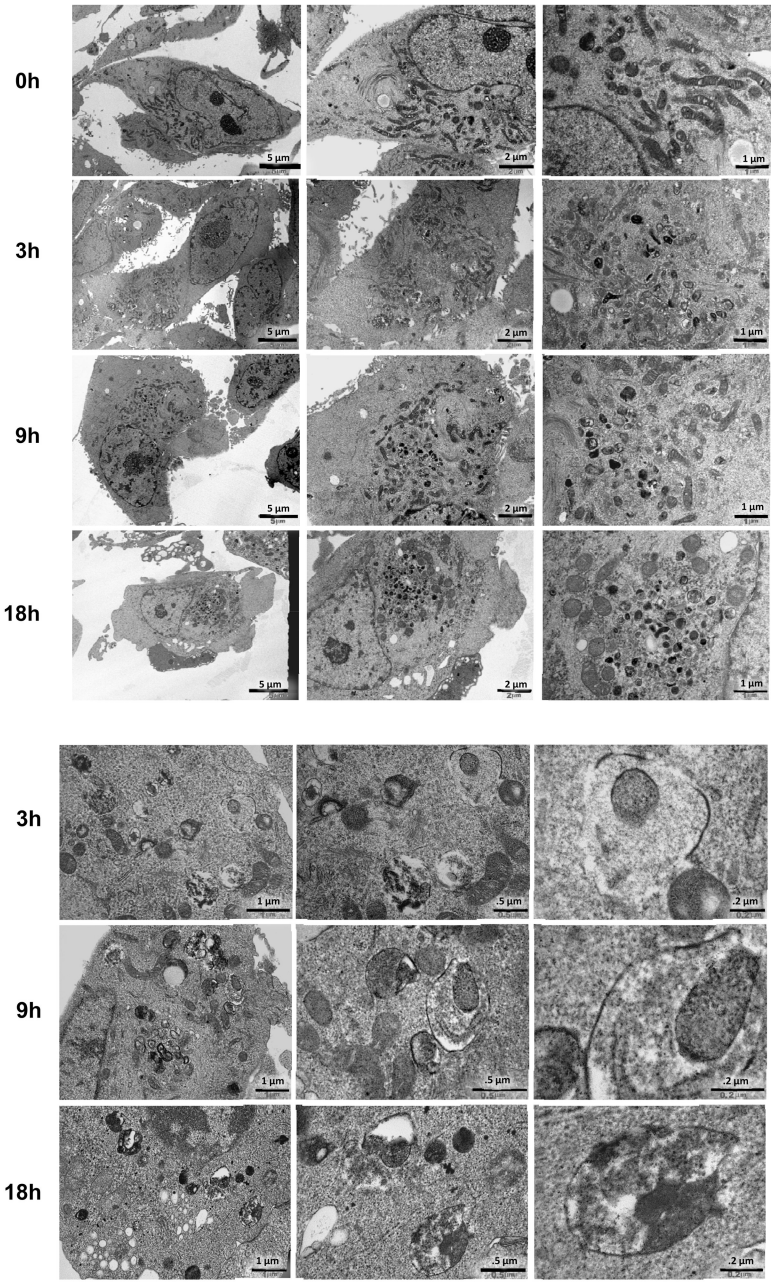

Figure 3.

As_2O_3 induces autophagy in ovarian cells. **(a)** T80 (left panel), HEY (middle panel), and SKOV3 (right panel) cells were seeded at 250,000 cells per well in 6-well plates. After overnight attachment, the cells were treated with varying concentrations of As_2O_3 (2–50μM). After 18 hour incubation, the cell lysates were harvested and western analysis was performed using the following antibodies: (1) SnoN, (2) PARP, (3) Procaspase-3, (4) LC3, (5) p62, and (6) GAPDH as a loading control. The data shown are representative of 3 independent experiments. **(b)** HEY cells were plated at 250,000 cells per well in 6-well plate. After overnight attachment, cells were treated with 25μM As_2O_3 for varying times (0, 3, 9, 18, 24, and 30 hours) and light microscope images were captured at 40× magnification.

The data shown are representative images. **(c)** HEY cells were seeded at 250,000 cells per well. Following overnight attachment, the cells were treated with 25μM As_2O_3 at various time points (3, 9, 18, 24, 30h). Cell lysates were harvested and western analysis was performed using the following antibodies: (1) EVI1, (2) SnoN, (3) TAK1, (4) TGFβRII, (5) SMAD2/3, (6) PARP, (7) Procaspase-3, (8) LC3, (9) Beclin-1, (10) p62, and (11) GAPDH as a loading control. The data shown are representative of 2 independent experiments. **(d)** and **(e)**, Confluent HEY cells grown in T-75 flasks were treated with 25μM As_2O_3 for 3, 9, 18 hours and prepared for TEM. Images were captured at varying magnifications as indicated. Representative images are shown.

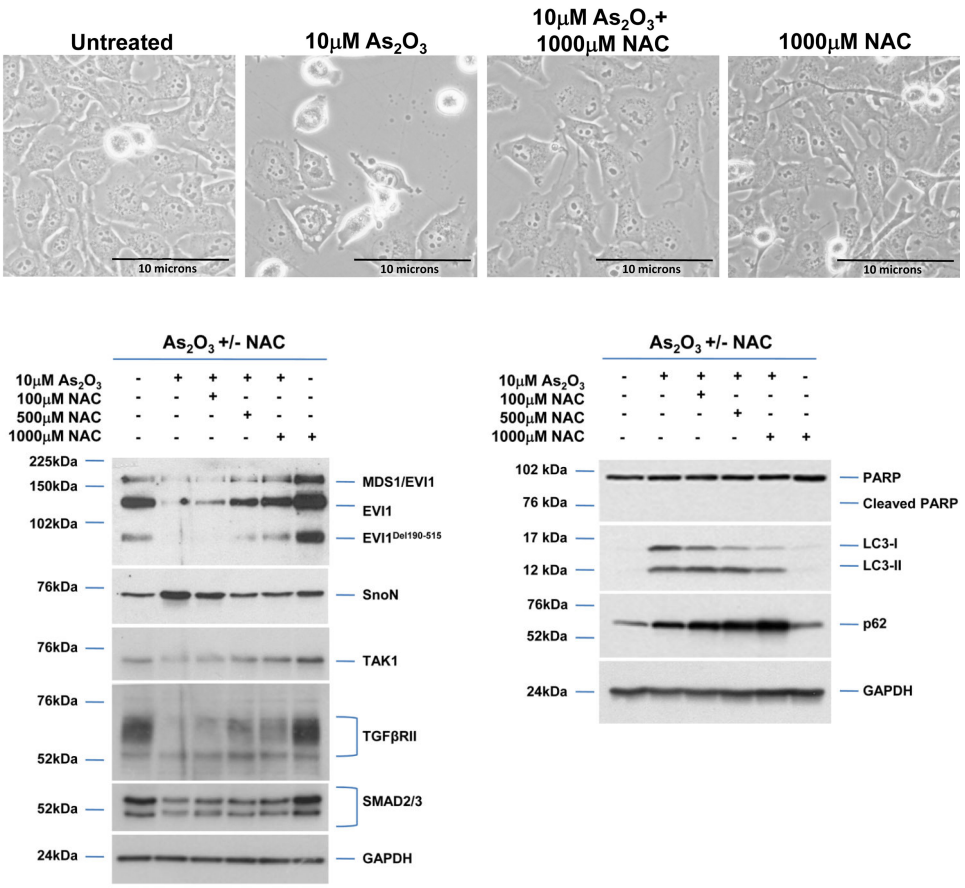

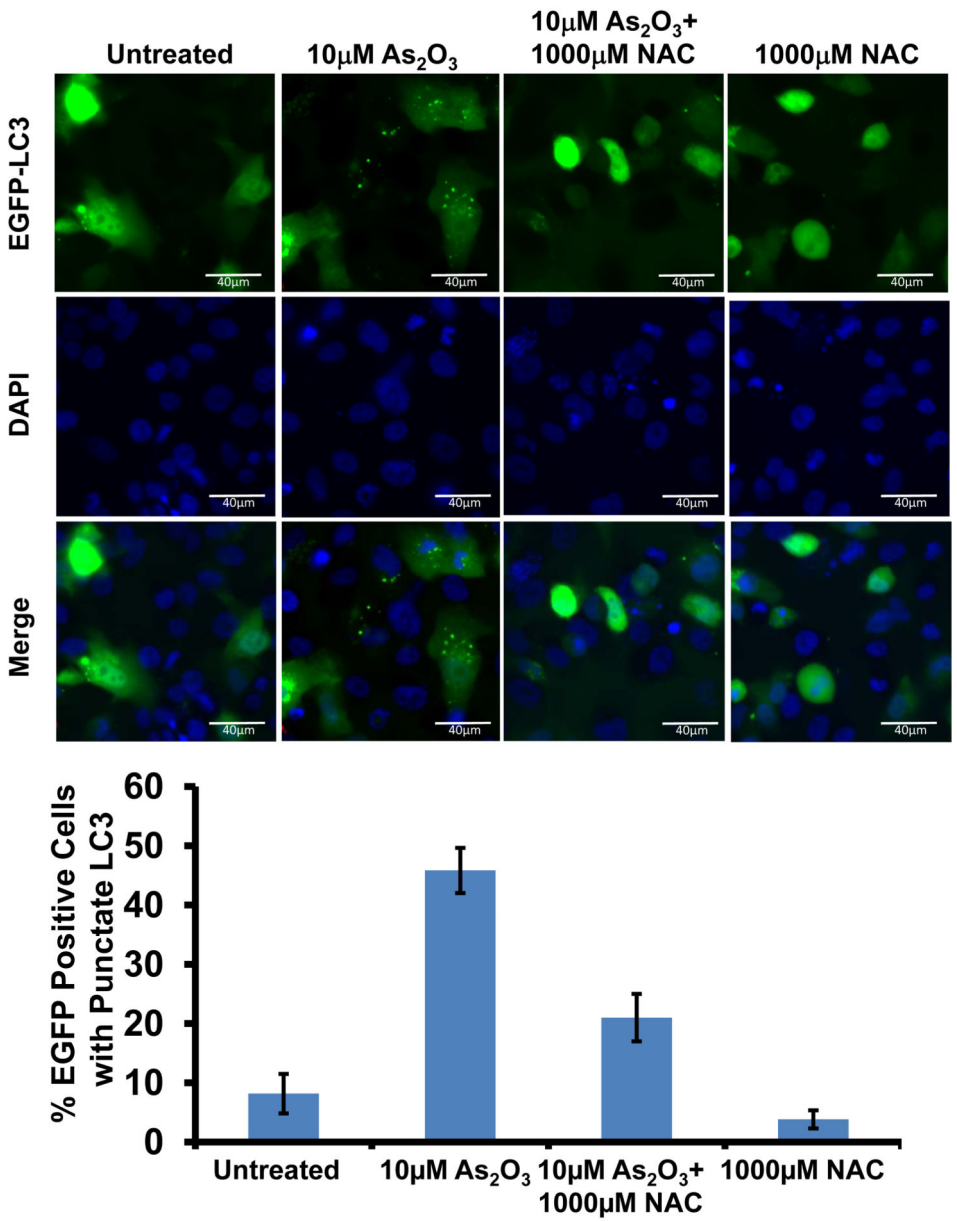

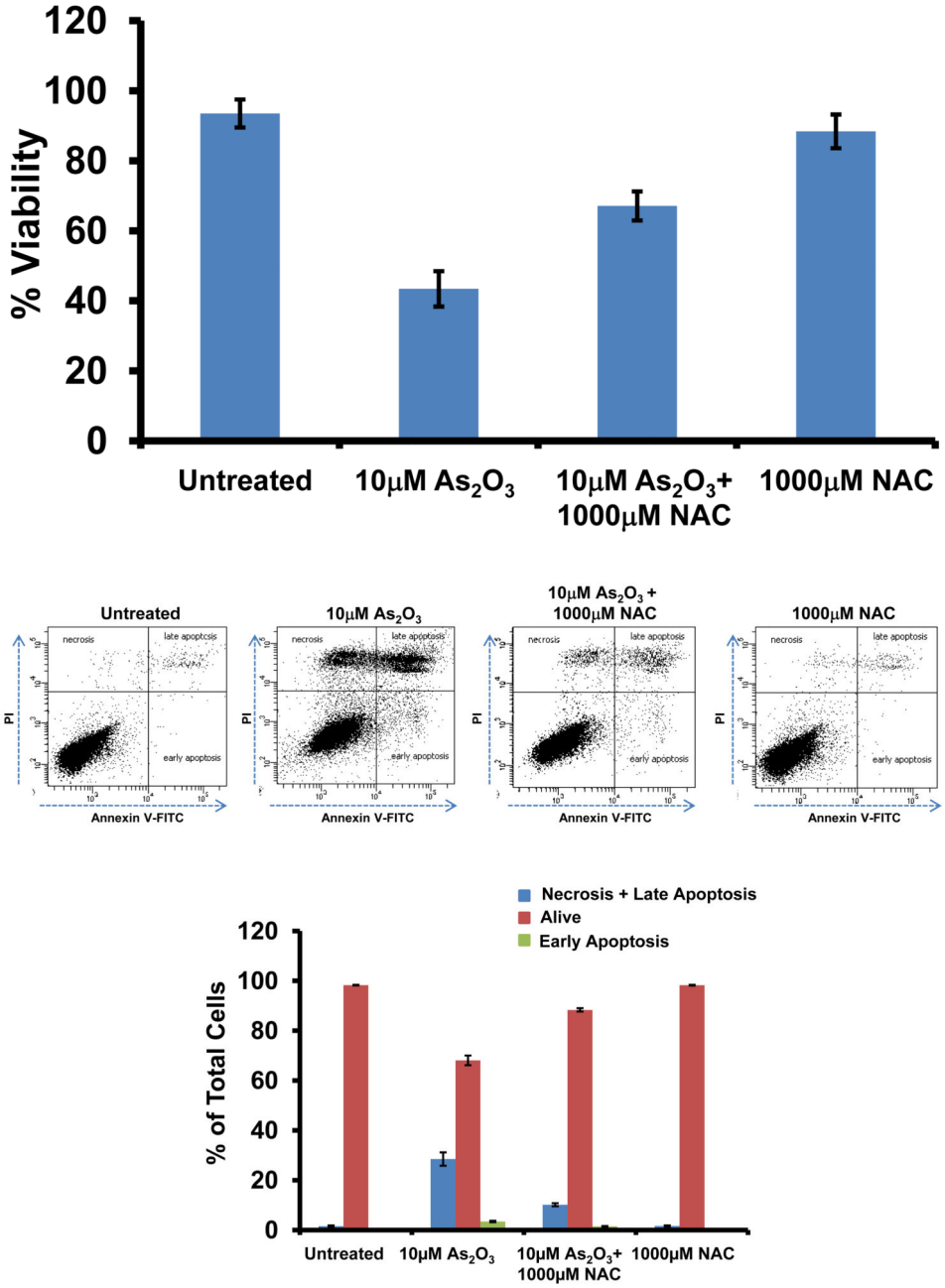

Figure 4.

Effects of As_2O_3 are reversed by antioxidant. **(a)** HEY cells were seeded at 250,000 cells per well in a 6-well plate. Following 24 hours, cells were treated with (1) 10μM As_2O_3, (2) 1000μM NAC, or (3) 10μM As_2O_3, and 1000μM NAC. After 18 hour incubation, the cells were photographed using a light microscope at 40× magnification. The data shown are representative images. **(b)** HEY cells were seeded at 250,000 cells per well in a 6-well plate. Following 24 hour cell attachment, cells were treated with (1) 10μM As_2O_3 alone, (2) 10μM As_2O_3 with 100μM NAC, (3) 10μM As_2O_3 with 500μM NAC, (4) 10μM As_2O_3 with 1000μM NAC, or (5) 1000μM NAC only. Following 18 hours incubation, cell lysates were

harvested and western analysis was performed using the following antibodies (left panel): (1) EVI1, (2) SnoN, (3) TAK1, (4) TGFβRII, (5) SMAD2/3, and (6) GAPDH as a loading control as well as (right panel): (1) PARP, (2) LC3, (3) p62, and (4) GAPDH. The data shown are representative of 3 independent experiments. **(c)** HEY cells were plated at 250,000 cells per well in 6-well plate onto glass coverslips. After overnight attachment, cells were transfected with EGFP-LC3. Following recovery for 24 hours, cells were treated with: (1) 10μM As_2O_3, (2) 10μM As_2O_3 and 1000μM NAC, or (3) 1000μM NAC for 18 hours. (Top panel) Immunofluorescence images were obtained at 40× magnification. (Bottom panel) The displayed graph is the quantification of the data presented as the percentage of EGFP positive cells with punctate LC3 expression. The data shown are representative of 2 independent experiments. **(d)** Cell viability was assessed using the CellTiter-Glo assay in HEY cells treated for 18 hours with 10μM As_2O_3 in the absence or presence of 1000μM NAC or 1000μM NAC alone. Results are presented as % cell viability relative to control cells. The data shown are representative of 3 independent experiments. **(e)** (Top panel) HEY cells were seeded at 250,000 cells per well in 6-well plates. Following cell attachment, cells were treated with (1) 10μM As_2O_3, (2) 10μM As_2O_3 and 1000μM NAC, and (3) 1000μM NAC, at which time both the floating and adherent cells were collected. Cells were stained with annexin V-FITC and propidium iodide (PI) followed by flow cytometric analysis. Raw data plots are shown as log fluorescence values of annexin V-FITC and PI on the X and Y axis, respectively. (Bottom panel) The data is also displayed in a bar graph as the percentage of viable, early apoptotic, and late apoptotic/necrotic cells. The data shown are representative of 3 independent experiments.

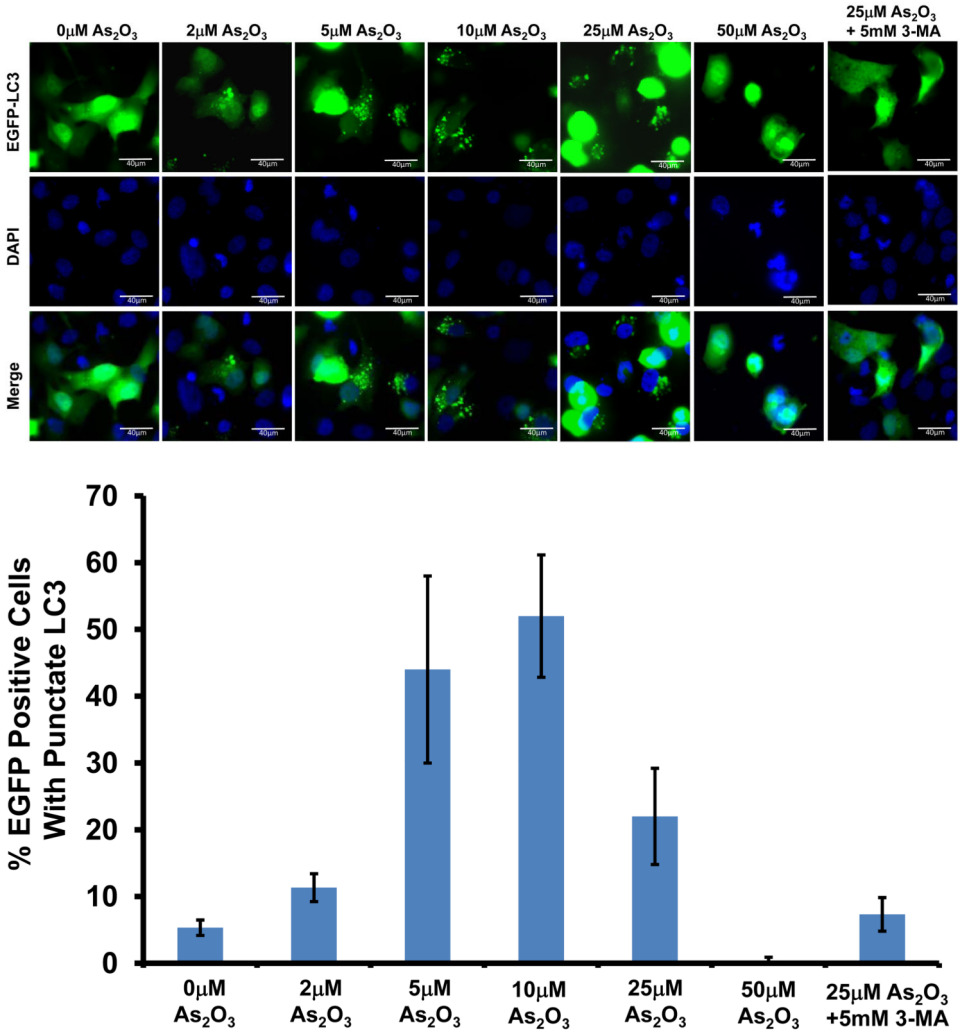

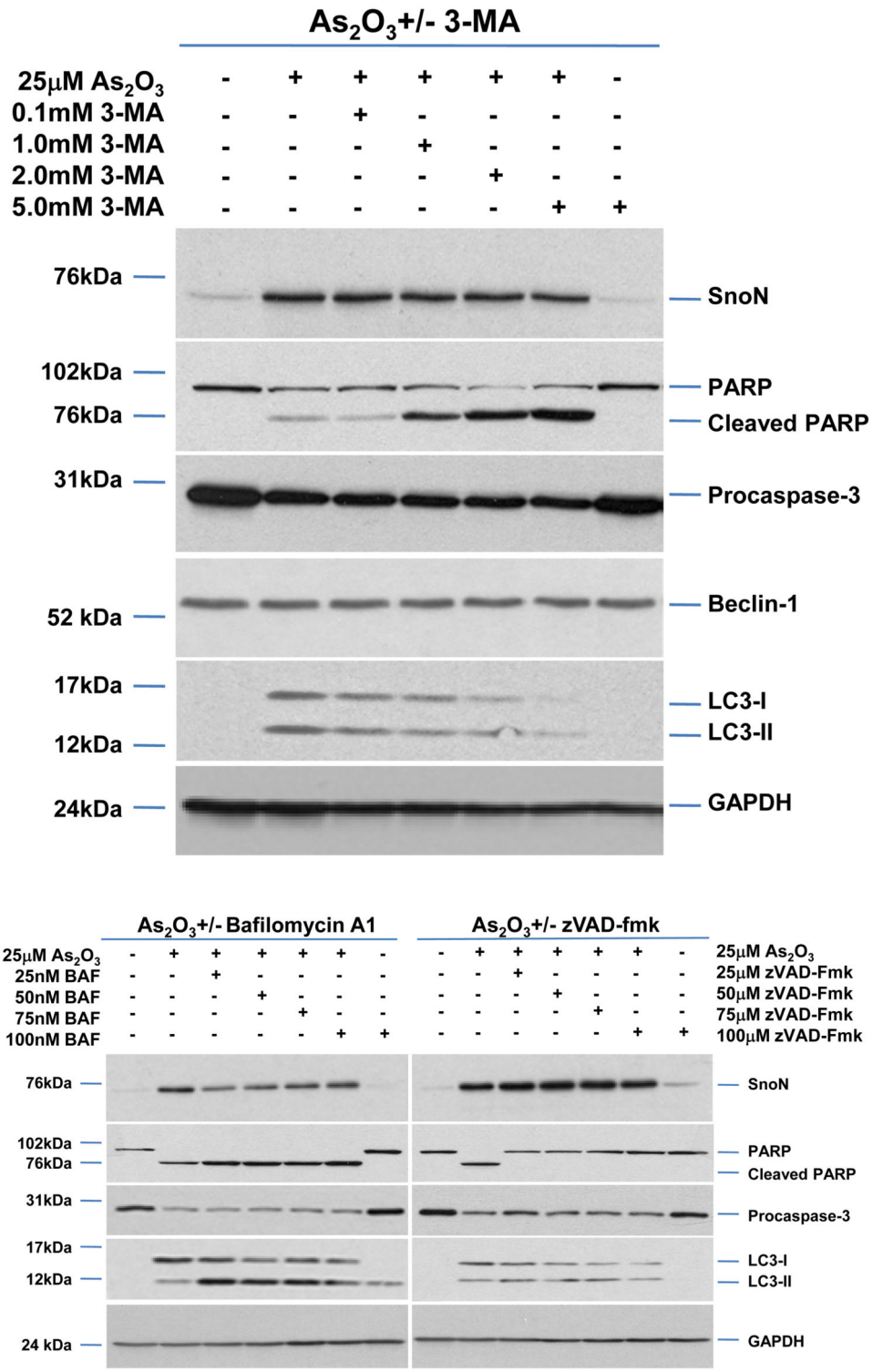

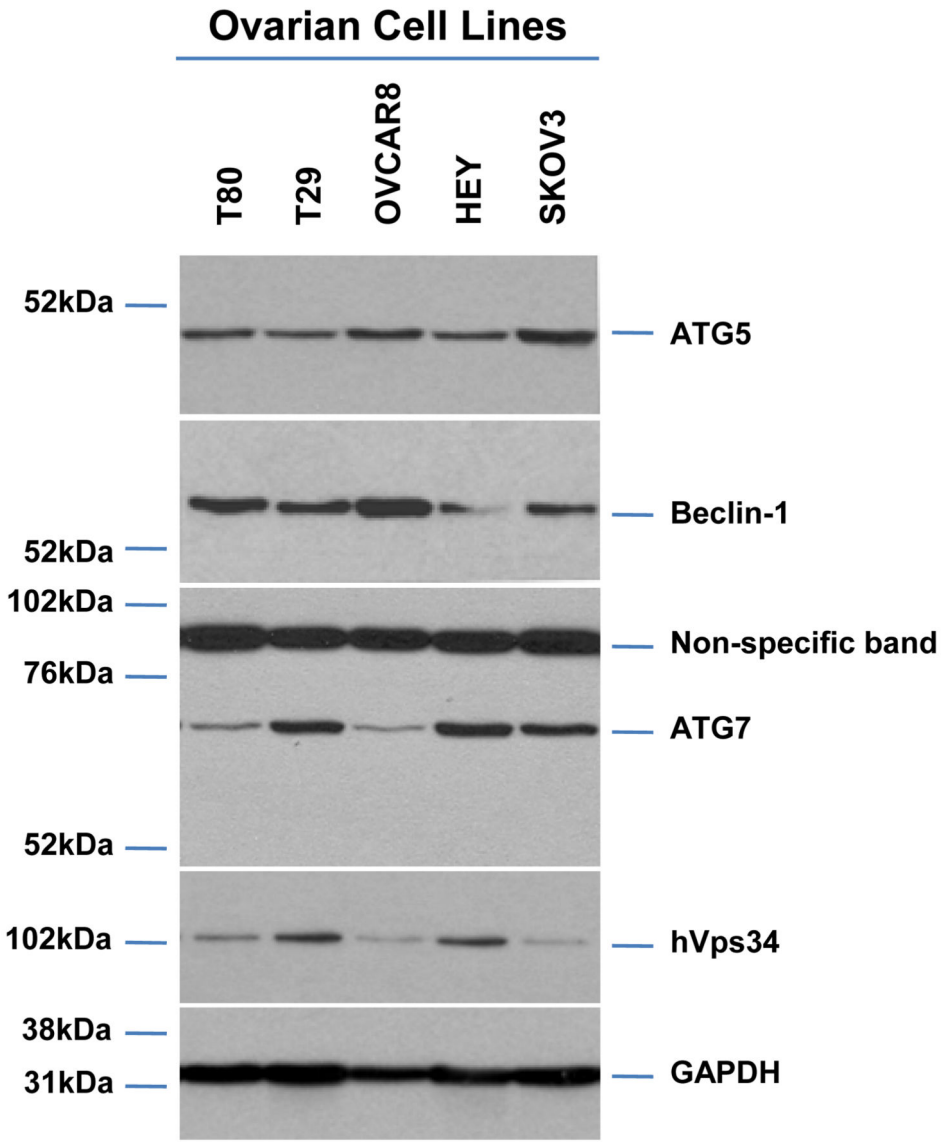

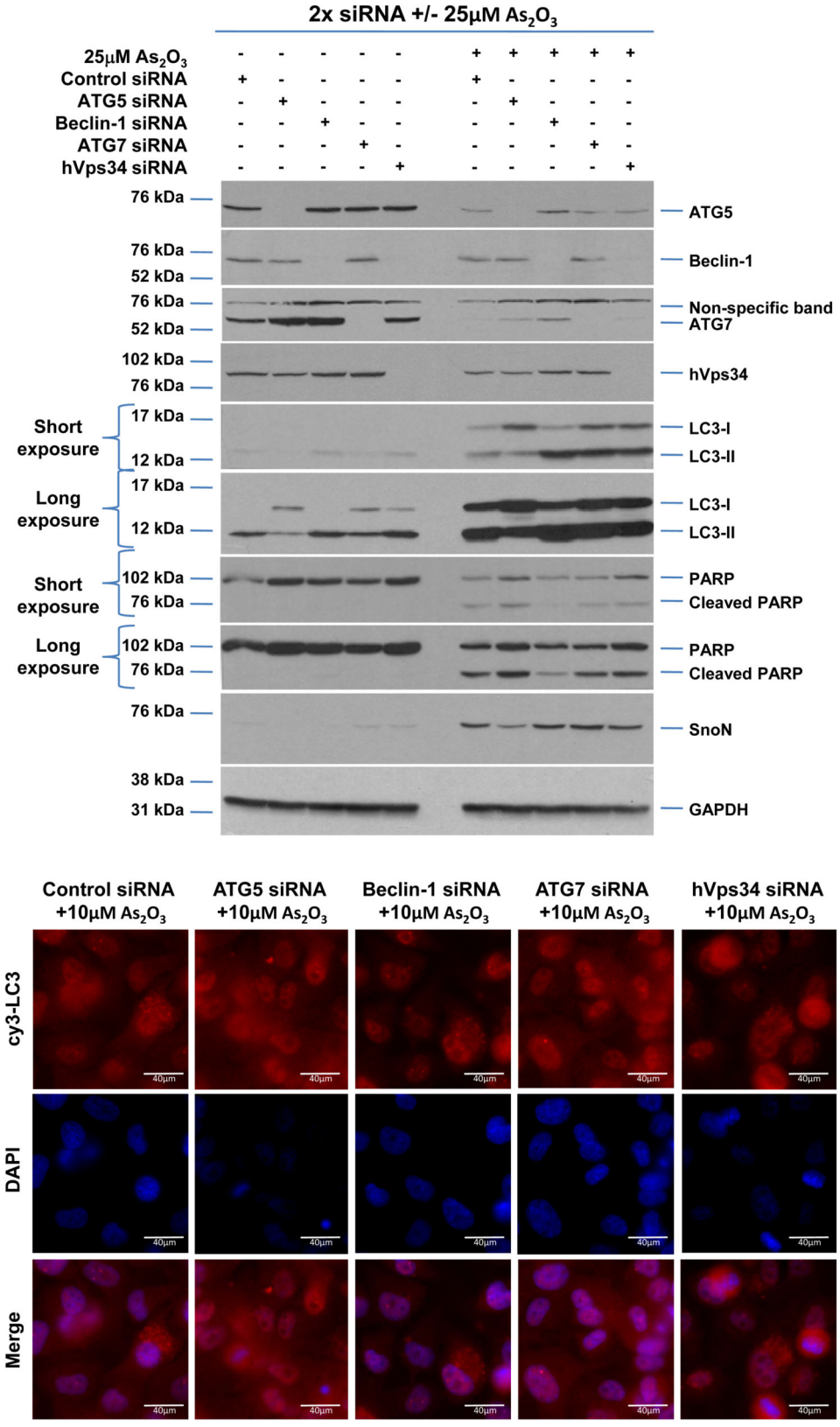

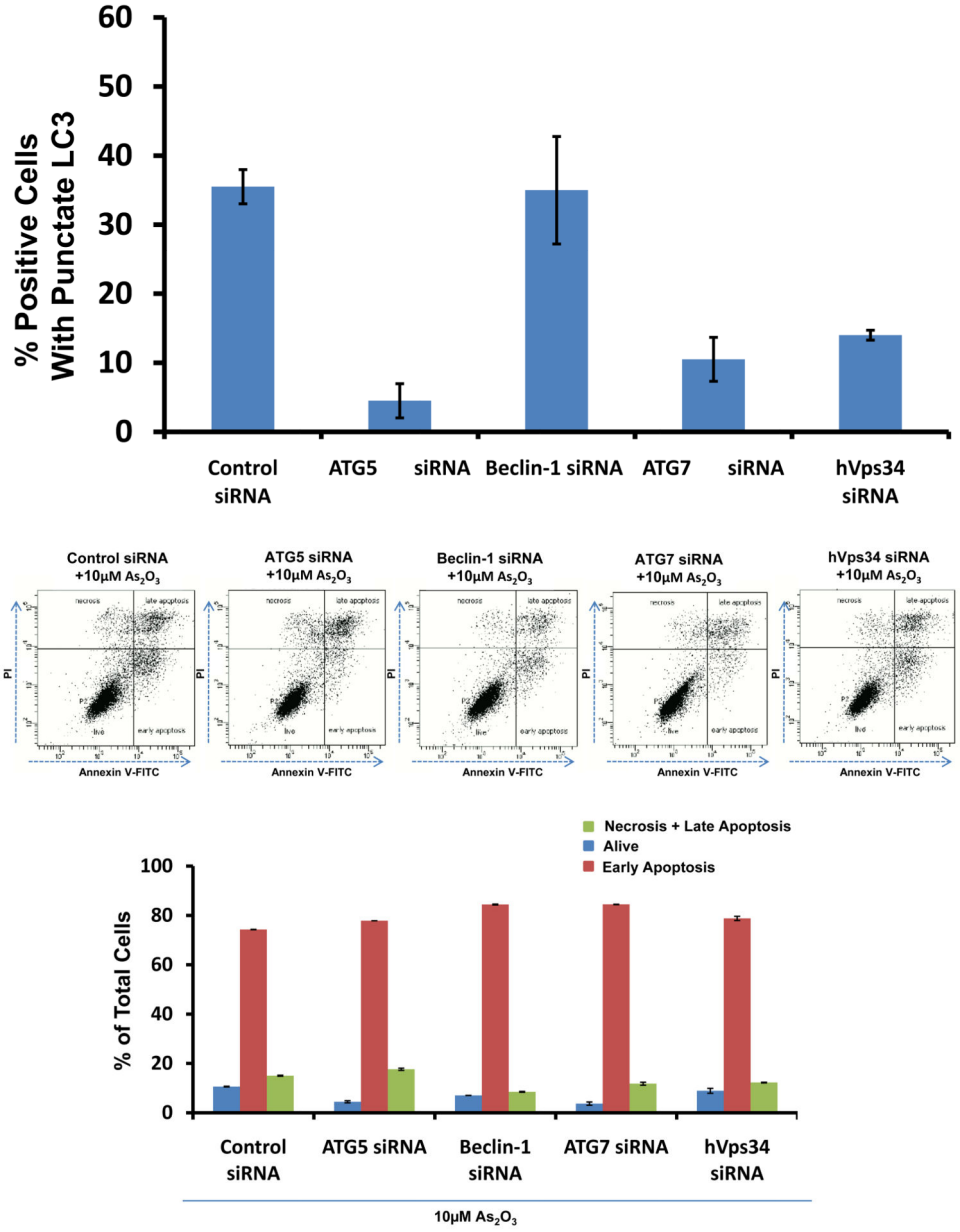

Figure 5.

As_2O_3 induces autophagy via a Beclin-1 independent pathway. **(a)** HEY cells were plated at 250,000 cells per well in 6-well plate onto glass coverslips. After overnight attachment, cells were transfected with EGFP-LC3. Following recovery for 24 hours, cells were treated with increasing doses of As_2O_3 (2–50μM) or 25μM As_2O_3 in the presence of 5mM 3-MA for 18 hours. Immunofluorescence images were obtained at 40× magnification. The data shown are representative of 2 independent experiments. **(b)** Immunofluorescence data from **(a)** was quantitated and presented as the percentage of EGFP positive cells with punctate LC3 expression. **(c)** HEY cells were seeded at 250,000 cells per well. After 24 hours, the cells were treated with: (1) 25μM As_2O_3, (2) 25μM As_2O_3 and 0.1mM 3-MA, (3) 25μM As_2O_3 and 1.0mM 3-MA, (4) 25μM As_2O_3 and 2.0mM 3-MA, (5) 25μM As_2O_3 and 5.0mM 3-MA,

and (6) 5.0mM 3-MA only for 18 hours. Cell lysates were harvested and western analysis was performed using the following antibodies: (1) SnoN, (2) PARP, (3) Procaspase-3, (4) Beclin-1, (5) LC3, and (6) GAPDH as a loading control. The data shown are representative of 4 independent experiments. **(d)** HEY cells were seeded at 250,000 cells per well. (Left panel): Following overnight attachment, the cells were treated with: (1) 25μM As_2O_3 (2) 25μM As_2O_3 and 25nM Bafilomycin A (BAF), (3) 25μM As_2O_3 and 50nM Bafilomycin A, (4) 25μM As_2O_3 and 75nM Bafilomycin A, (5) 25μM As_2O_3 and 100nM Bafilomycin A, and (6) 100nM Bafilomycin A only. (Right panel): After 24 hours, the cells were treated with: (1) 25μM As_2O_3, (2) 25μM As_2O_3 and 25μM zVAD-Fmk (3) 25μM As_2O_3 and 50μM zVAD-Fmk (4) 25μM As_2O_3 and 75μM zVAD-Fmk (5) 25μM As_2O_3 and 100μM zVAD-Fmk, and (6) 100μM zVAD-Fmk only. After 18 hour incubation, cell lysates were harvested and western analysis was performed using the following antibodies: (1) SnoN, (2) PARP, (3) Procaspase-3, (4) LC3, and (5) GAPDH as a loading control. The data shown are representative of 2 independent experiments. **(e)** Ovarian cells (T80, T29, OVCAR8, HEY, and SKOV3 cells) were seeded at 500,000 cells per well in T25 flasks. After overnight attachment, cell lysates were harvested and western analysis was performed using the following antibodies: (1) ATG5, (2) Beclin-1, (3) ATG7, (4) (5) hVps34, and (6) GAPDH as a loading control. **(f)** HEY cells were seeded at 250,000 cells per well in 6-well plates. After 24 and 48 hours, the cells were treated with (1) non-targeting (control) siRNA, (2) ATG5 siRNA, (3) Beclin-1 siRNA, (4) ATG7 siRNA, and (5) hVps34 siRNA. Seventy-two hours post-transfection, cells were treated for 18 hours with 25μM As_2O_3. Cell lysates were harvested and western analysis was performed using the following antibodies: (1) ATG5, (2) Beclin-1, (3) ATG7, (4) hVps34, (5) LC3, (6) PARP, (7) SnoN, and (8) GAPDH as a loading control. The data shown are representative of 2 independent experiments. **(g)** HEY cells were seeded at 250,000 cells per well in 6-well plates. After 24 and 28 hours, the cells were treated with (1) non-targeting (control) siRNA, (2) ATG5 siRNA, (3) Beclin-1 siRNA, (4) ATG7 siRNA, and (5) hVps34 siRNA. Seventy-two hours post-transfection, cells were treated for 24 hours with 10μM As_2O_3. Cells were stained with LC3B rabbit polyclonal antibody and counterstained with DAPI. Immunofluorescence images are representative and were obtained at 63× magnification. **(h)** Immunofluorescence data was quantitated and presented as the percentage of positive cells with punctate LC3 expression. The data shown are representative of 2 independent experiments. **(i)** HEY cells were seeded at 250,000 cells per well in 6-well plates. After 24 and 28 hours, the cells were treated with (1) non-targeting (control) siRNA, (2) ATG5 siRNA, (3) Beclin-1 siRNA, (4) ATG7 siRNA, and (5) hVps34 siRNA. Seventy-two hours post-transfection, cells were treated for 48 hours with 10μM As_2O_3 at which time both the floating and adherent cells were collected. Cells were stained with annexin V-FITC and propidium iodide (PI) followed by flow cytometric analysis. Raw data plots are shown as log fluorescence values of annexin V-FITC and PI on the X and Y axis, respectively (Top panel). The data is also displayed as a bar graph as the percentage of viable, early apoptotic, and late apoptotic/necrotic cells. The data shown are representative of 2 independent experiments (bottom panel).

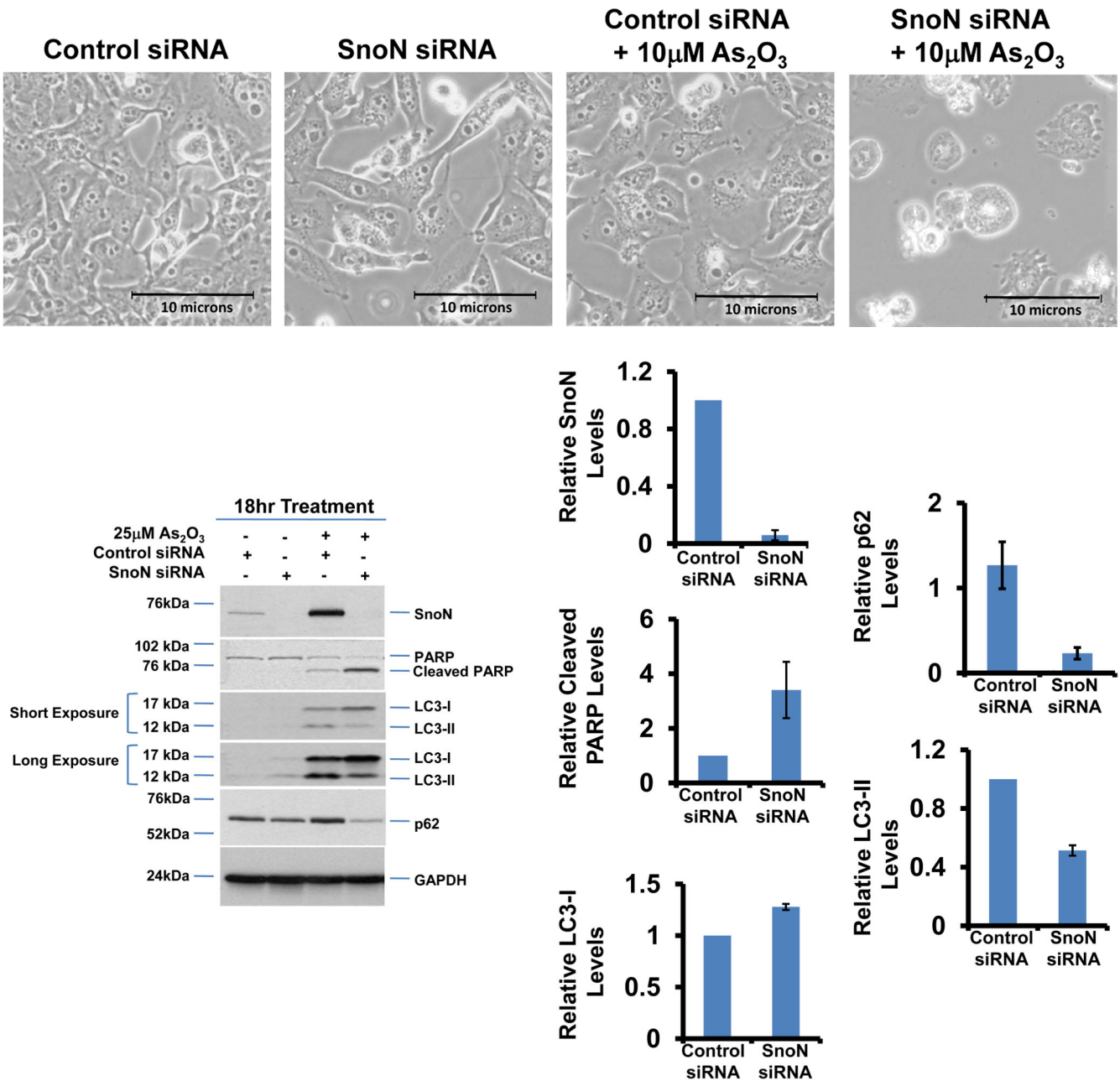

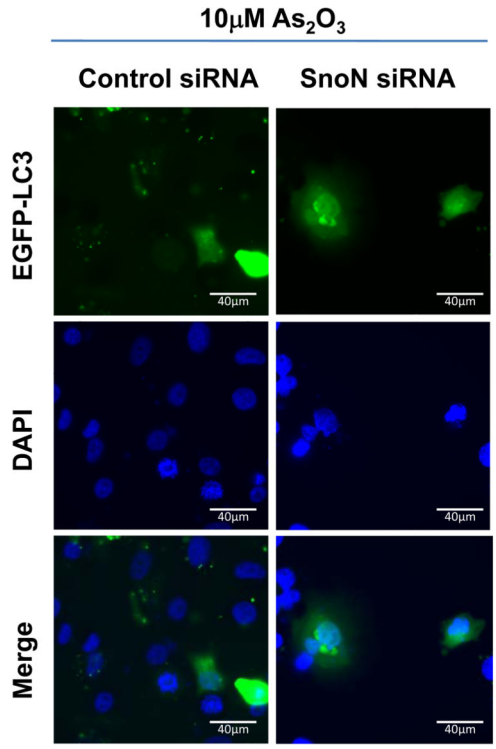

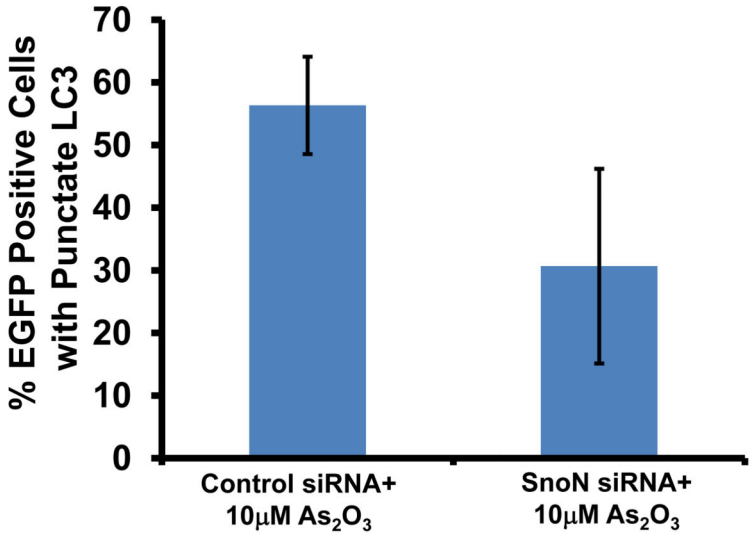

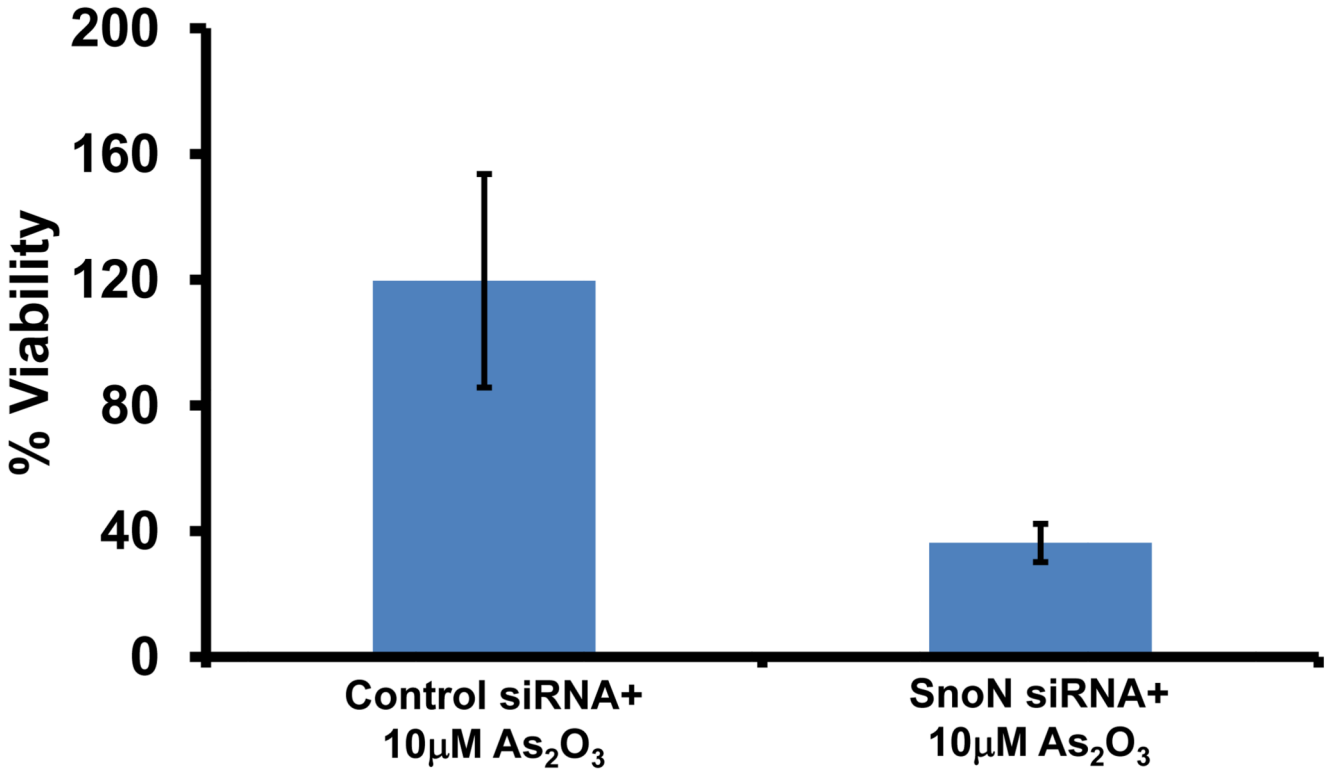

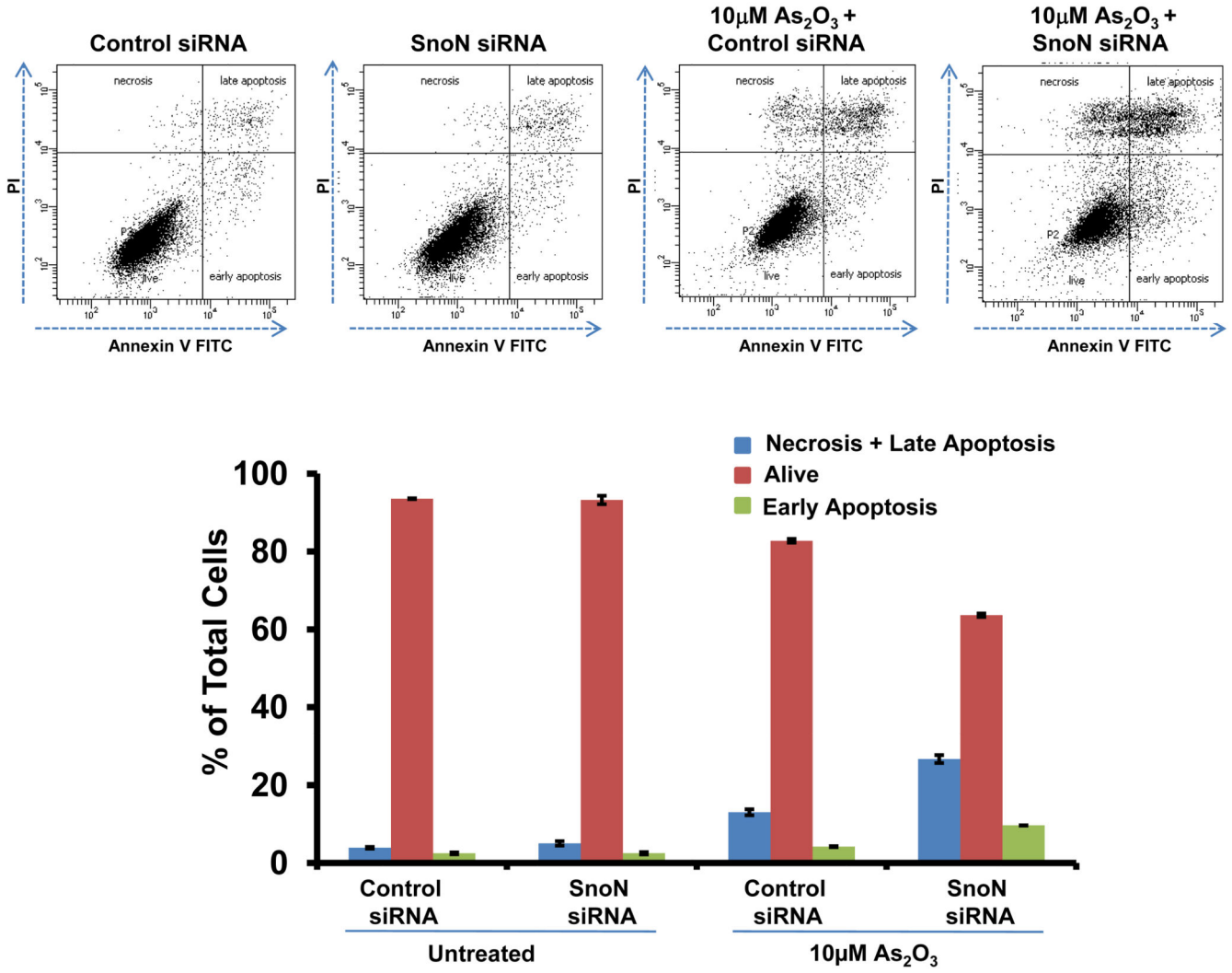

Figure 6.

Knockdown of SnoN modulates the sensitivity of ovarian cancer cells to As_2O_3. **(a)** HEY cells were plated at 250,000 cells per well in 6-well plate. After overnight attachment, the cells were transiently transfected with (1) non-targeting (control) siRNA or (2) SnoN siRNA. Following 24 hours post-transfection, the cells were treated with 10μM As_2O_3. After 18 hours, light microscope images were captured at 40× magnification. The data shown are representative images. **(b)** (Left panel) HEY cells were seeded at 250,000 cells per well in 6-well plates. After 24 hours, the cells were transiently transfected with (1) non-targeting (control) siRNA or (2) SnoN siRNA. Following 24 hours post-transfection, the cells were treated with 25μM As_2O_3. After 18 hour incubation, cell lysates were harvested and western analysis was performed using the following antibodies: (1) SnoN, (2) PARP, (3) LC3, (4) p62, and (4) GAPDH as a loading control. The data shown are representative of 2 independent experiments. (Right panel) Densitometric analyses of selected western data (only As_2O_3-treated samples) which include SnoN, cleaved PARP, LC3-I, LC3-II, and p62. **(c)** (Left panel) HEY cells were plated at 250,000 cells per well in 6-well plate onto glass coverslips. After overnight attachment, cells were transfected with EGFP-LC3. Following

recovery for 24 hours, cells were treated with (1) non-targeting (control) siRNA or (2) SnoN siRNA followed by cell treatment with 10μM As_2O_3. Immunofluorescence images are representative and were obtained at 40× magnification. (Right panel) Immunofluorescence data was quantitated and presented as the percentage of EGFP positive cells with punctate LC3 expression. The data shown are representative of 2 independent experiments. **(d)** Cell viability was assessed using the CellTiter-Glo assay in HEY cells transfected with control or SnoN siRNA followed by treatment for 18 hours with 10μM As_2O_3. Results are presented as % cell viability relative to non-targeting (control) siRNA treated cells. The data shown are representative of 2 independent experiments. **(e)** (Top panel) HEY cells were seeded at 250,000 cells per well in 6-well plates. Following 24 hours, cells were treated with (1) non-targeting (control) siRNA or (2) SnoN siRNA. Twenty-four hours post-transfection, cells were treated for 48 hours with 10μM As_2O_3 at which time both the floating and adherent cells were collected. Cells were stained with annexin V-FITC and propidium iodide (PI) followed by flow cytometric analysis. Raw data plots are shown as log fluorescence values of annexin V-FITC and PI on the X and Y axis, respectively. (Bottom panel) The data is displayed in a bar graph as the percentage of viable, early apoptotic, and late apoptotic/ necrotic cells. The data shown are representative of 3 independent experiments.

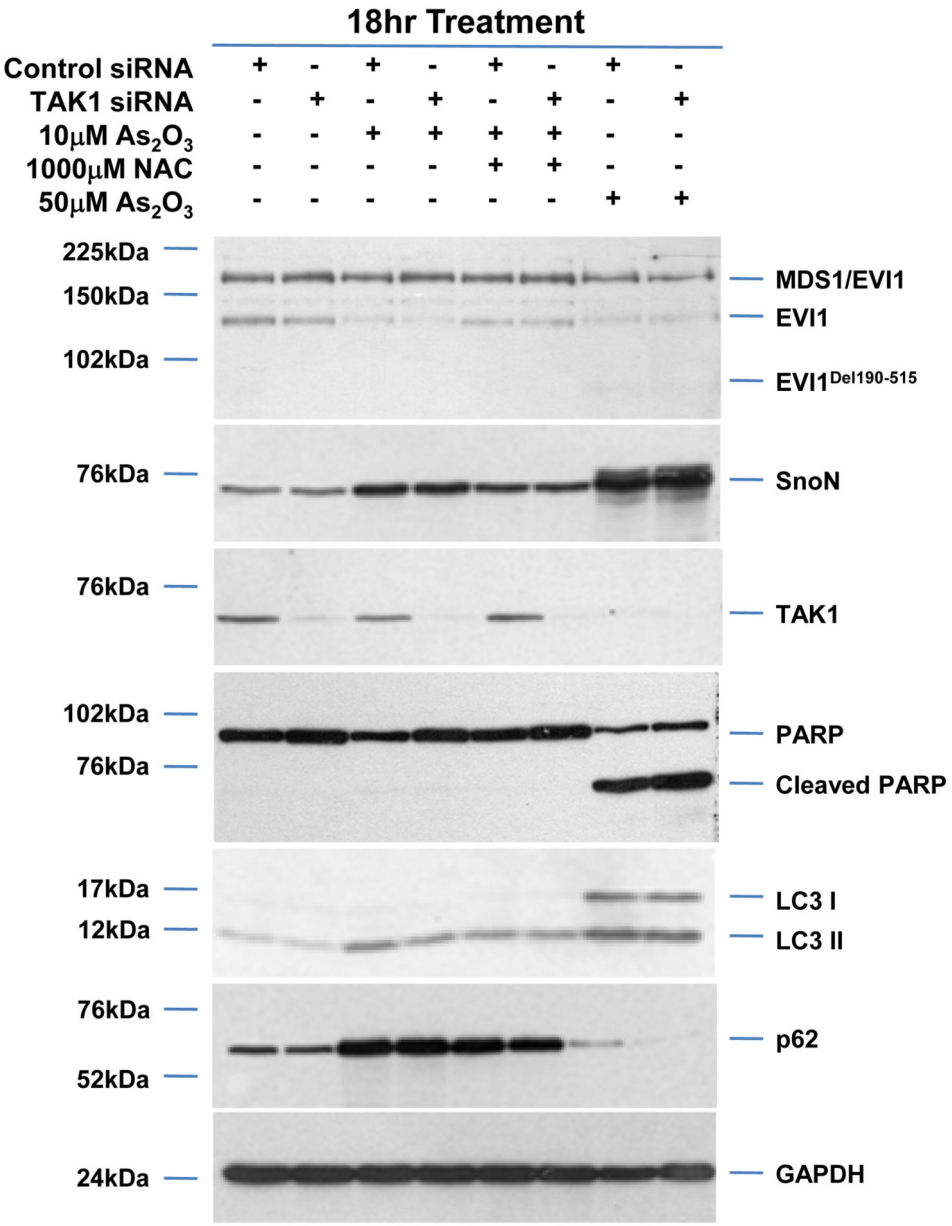

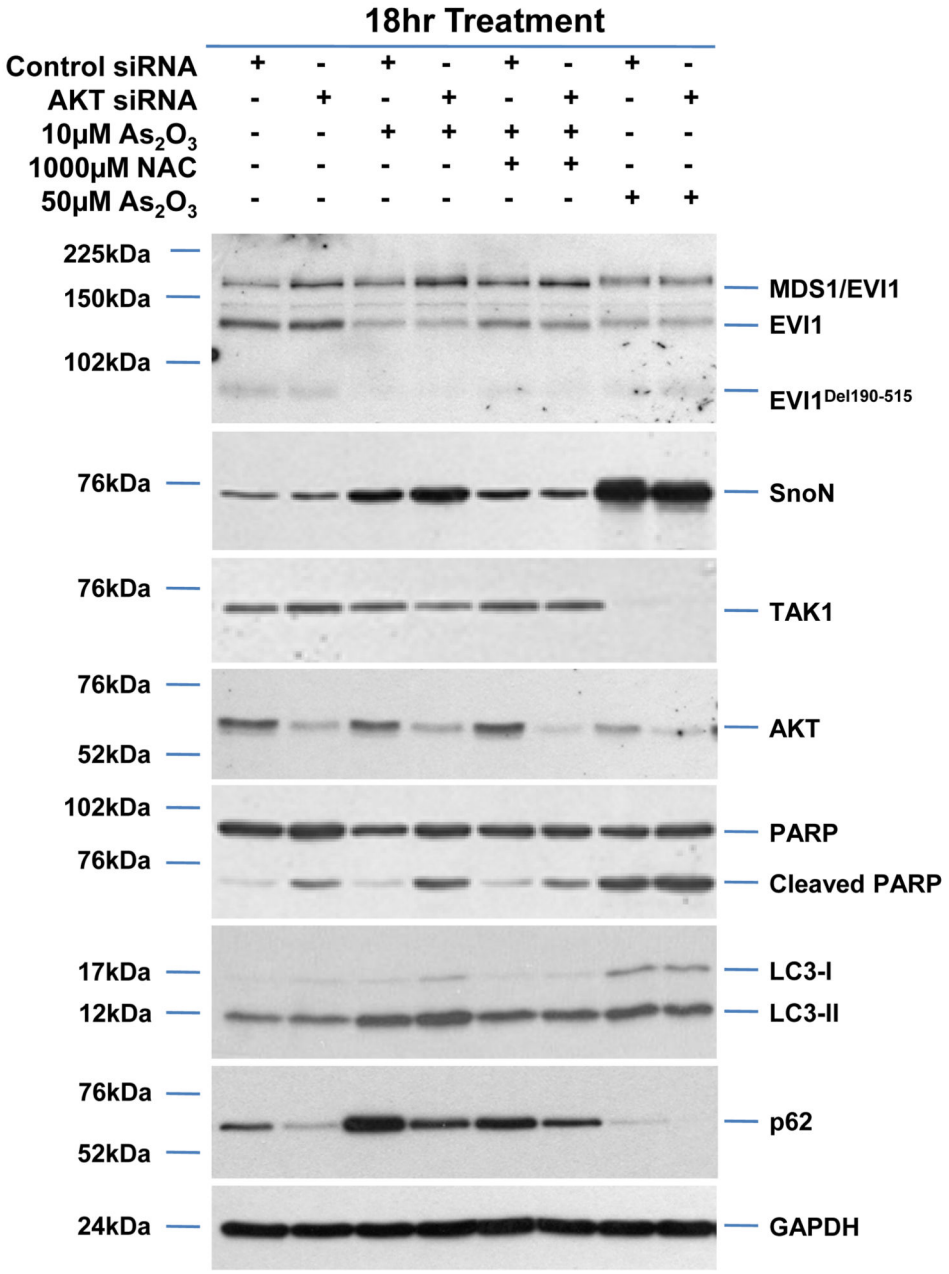

Figure 7.

AKT knockdown modulates apoptosis in response to As_2O_3. **(a)** HEY cells were seeded at 375,000 cells per well in 6-well plates. Following 24 hour attachment, cells were transfected with either non-targeting (control) or TAK1 siRNA. Transfected cells were then treated for 18 hours with (1) 10μM As_2O_3, (2) 10μM As_2O_3 with 1mM NAC, and (3) 50μM As_2O_3. Cell lysates were harvested and western analysis was performed using the following antibodies (1) EVI1, (2) SnoN, (3) TAK1, (4) PARP, (5) LC3, (6) p62, and (7) GAPDH as a loading control. The data shown are representative of 2 independent experiments. **(b)** HEY cells were seeded at 375,000 cells per well in 6-well plates. Following 24 hour attachment, cells were transfected with either non-targeting (control) or AKT siRNA. Transfected cells

were then treated for 18 hours with (1) 10μM As_2O_3, (2) 10μM As_2O_3 with 1mM NAC, and (3) 50μM As_2O_3. Cell lysates were harvested and western analysis was performed using the following antibodies: (1) EVI1, (2) SnoN, (3) TAK1, (4) AKT, (5) PARP, (6) LC3, (7) p62, and (8) GAPDH as a loading control. The data shown are representative of 2 independent experiments.

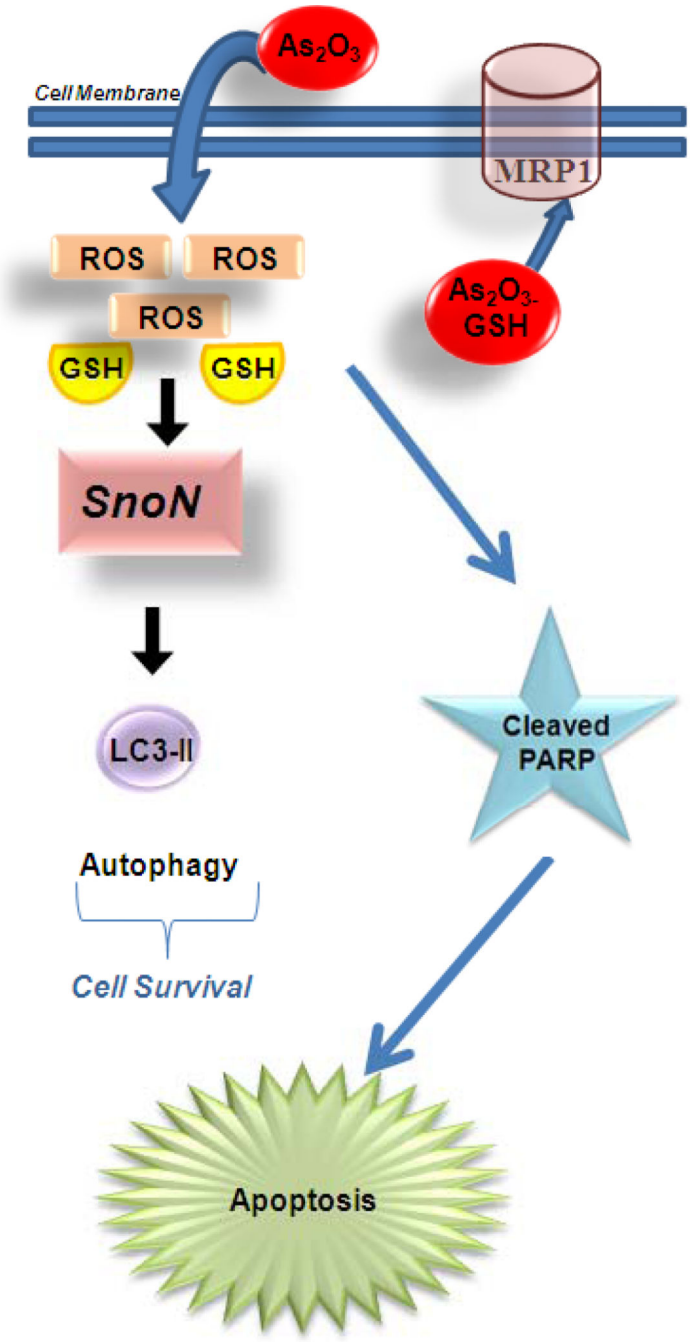

Figure 8.

Therapeutic potential for SnoN in mediating As_2O_3-induced autophagic cell survival. As_2O_3 diffuses into the cell through the cell membrane leading to a reduction in intracellular glutathione (GSH) levels and an increase in reactive oxygen species (ROS) which through unknown mechanisms lead to increases in SnoN levels. SnoN alters LC3-II expression, a marker of autophagosome maturation, suggesting that SnoN can induce autophagy. Induction of autophagy appears to be a protective mechanism of cell survival following

As_2O_3 treatment in ovarian cells. In high MRP1 expressing cell lines, As_2O_3 is effluxed through these channels resulting in reduced sensitivity to As_2O_3-induced apoptosis.